Inorg. Chem. **2009**, *48*, 1005−1017

Supersilylated Tetraphosphene Derivatives $M_2[t\text{-}Bu_3SiPPPPSi\text{-}t\text{-}Bu_3]$ (M = Li, Na, Rb, Cs) and $Ba[t\text{-}Bu_3SiPPPPSi\text{-}t\text{-}Bu_3]$: Reactivity and Cis−Trans Isomerization

Andreas Lorbach,[†] Andor Nadj,[†] Sandor Tüllmann,[†] Franz Dornhaus,[†] Frauke Schödel,[†] Inge Sänger,[†] Günter Margraf,[†] Jan W. Bats,[‡] Michael Bolte,[†] Max C. Holthausen,[†] Matthias Wagner,[†] and Hans-Wolfram Lerner*[,†]

Institut für Anorganische Chemie and Institut für Organische Chemie, Goethe-Universität Frankfurt am Main, Max-von-Laue-Strasse 7, 60438 Frankfurt am Main, Germany

Received August 22, 2008

The tetraphosphenediides $M_2[t\text{-}Bu_3SiPPPPSi\text{-}t\text{-}Bu_3]$ (M = Li, Na, K) were accessible by the reaction of P_4 with the silanides $M[Si\text{-}t\text{-}Bu_3]$ (M = Li, Na, K), whereas $M_2[t\text{-}Bu_3SiPPPPSi\text{-}t\text{-}Bu_3]$ (M = Rb, Cs) were obtained from the reaction of RbCl and CsF with $Na_2[t\text{-}Bu_3SiPPPPSi\text{-}t\text{-}Bu_3]$. ^{31}P NMR experiments revealed that, in tetrahydrofuran, $Na_2[t\text{-}Bu_3SiPPPPSi\text{-}t\text{-}Bu_3]$ adopts a cis configuration. However, treatment of $Na_2[t\text{-}Bu_3SiPPPPSi\text{-}t\text{-}Bu_3]$ with 18-crown-6 led to the formation of $[Na(18\text{-crown-}6)(thf)_2]_2[t\text{-}Bu_3SiPPPPSi\text{-}t\text{-}Bu_3]$ that possesses a trans configuration in the solid state. The ion-separated tetraphosphenediide $[Na(18\text{-crown-}6)(thf)_2]_2[t\text{-}Bu_3SiPPPPSi\text{-}t\text{-}Bu_3]$ was analyzed using X-ray crystallography (monoclinic, space group $P2_1/n$). The reaction of $Na_2[t\text{-}Bu_3SiPPPPSi\text{-}t\text{-}Bu_3]$ with BaI_2 gave, conveniently, the corresponding barium derivative $Ba[t\text{-}Bu_3SiPPPPSi\text{-}t\text{-}Bu_3]$. However, addition of AuI to the tetraphosphenediide $Na_2[t\text{-}Bu_3SiPPPPSi\text{-}t\text{-}Bu_3]$ yielded 1,3-diiodo-2,4-disupersilyl-cyclotetraphosphane (monoclinic, space group $C2/c$), which is an isomer of disupersilylated diiodotetraphosphene. A further isomeric derivative of disupersilylated tetraphosphene, the 3,5-disupersilyl-2,2-di-*tert*-butyl-2-stanna-bicyclo[2.1.$0^{1,4}$]pentaphosphane, which possesses a phosphanylcyclotriphosphane structure, was obtained by the reaction of $Na_2[t\text{-}Bu_3SiPPPPSi\text{-}t\text{-}Bu_3]$ with $t\text{-}Bu_2SnCl_2$. Calculations revealed that the acyclic cis and trans isomers of the dianions $[HPPPPH]^{2-}$ and $[H_3SiPPPPSiH_3]^{2-}$ are thermodynamically more stable than the cyclic isomers with a phosphanylcyclotriphosphane or a cyclotetraphosphane structure. However, the neutral cyclic isomers of H_4P_4 and $H_2(H_3Si)_2P_4$ represent more stable structures than the *cis*- and *trans*-tetraphosphenes $H_2P{-}P{=}P{-}PH_2$ and $(H_3Si)HP{-}P{=}P{-}PH(SiH_3)$, respectively. In addition, the molecular orbitals (MOs) of the silylated *cis*- and *trans*-tetraphosphene dianions of $[H_3SiPPPPSiH_3]^{2-}$, which are comparable with those of the ion-separated supersilylated tetraphosphenediide $[t\text{-}Bu_3SiPPPPSi\text{-}t\text{-}Bu_3]^{2-}$, show the highest occupied antibonding π^*MO (HOMO). The HOMO is represented by the $(p_z{-}p_z{+}p_z{-}p_z)$ π^* MO.

Introduction

The nitrogen compounds diazene HN=NH, triazene $HN{=}N{-}NH_2$, 2-tetrazene $H_2N{-}N{=}N{-}NH_2$, and their corresponding silyl derivatives with NN double bonds have been extensively studied.[1−10] In this context, it was reported that the unsaturated nitrogen−hydrogen compounds are temperature-sensitive (e.g., decomposition temperatures: −180 °C (HN=NH), −30 °C (*trans*-$H_2N{-}N{=}N{-}NH_2$)).[2,4] It was discovered that especially triazene $HN{=}N{-}NH_2$ and *cis*-2-tetrazene $H_2N{-}N{=}N{-}NH_2$ are very unstable (decomposition temperatures below −200 °C).[1,3] Generally, it was proved that their silyl derivatives are thermodynamically more stable than the unsaturated nitrogen−hydrogen compounds.[4−10] In the course of our investigation into tetrazenes, we were able to isolate several silylated tetrazene derivatives with cis configuration.[6−8] Up to now, knowledge about the chemistry of related unsaturated phosphorus compounds is rather

* To whom correspondence should be addressed. E-mail: lerner@chemie.uni-frankfurt.de.
[†] Institut für Anorganische Chemie. Fax: +49-69798-29260.
[‡] Institut für Organische Chemie.

(1) (a) Wiberg, N. *Adv. Organomet. Chem.* **1984**, *23*, 131. (b) Wiberg, N. *Adv. Organomet. Chem.* **1985**, *24*, 179.

10.1021/ic8016003 CCC: $40.75
Published on Web 12/23/2008

Scheme 1. P_4 Degradation with Silanides M[Si-*t*-Bu_3] (M = Na, K)

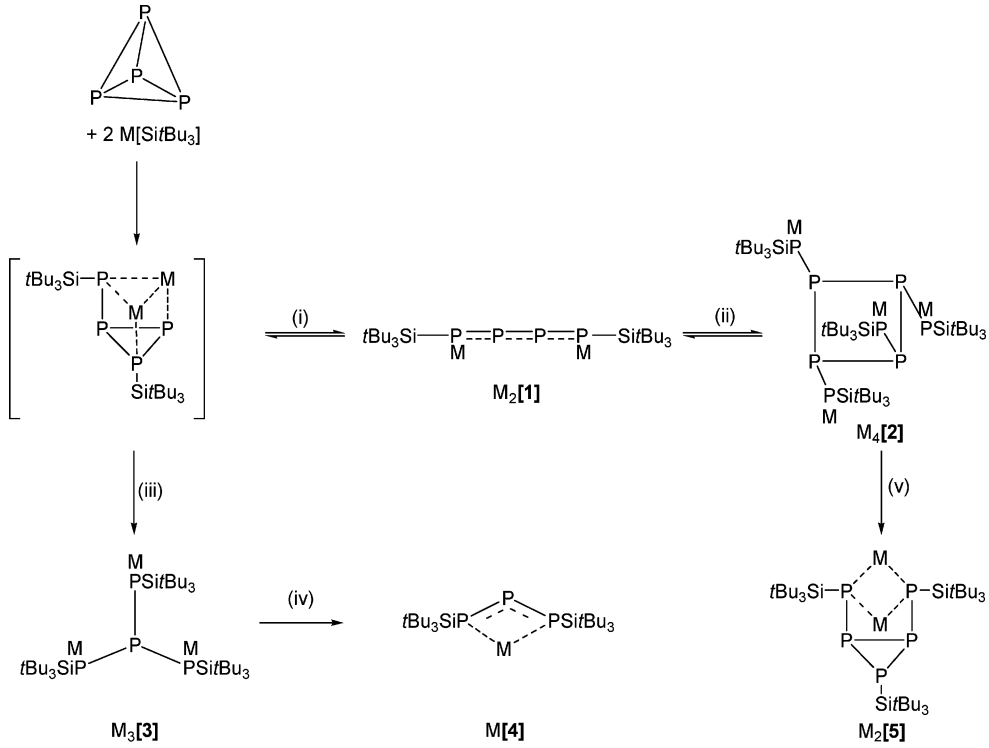

limited. In 1992, the synthesis and structure of the first structurally characterized tetraphosphene derivative with a P_4 chain were described (Figure 1).[11] The tetraphosphene **A** was prepared from $Li[(OC)_5CrP(SiMe_3)_2]$ and 1,2-dibromoethane in dimethoxyethane.[11] In 2005, P. P. Power and coworkers reported on the reaction of P_4 with dithallene $(TlAr)_2$ (Ar = C_6H_3-2,6-(C_6H_3-2,6-*i*-Pr_2)$_2$), which cleanly led to the formation of the tetraphosphene **B**.[12] Recently, in several reports, information about the reactivity of P_4 toward nucleophiles has been documented.[12−21] In this context, the tetraphosphene compounds **C** and **D** were synthesized from reactions of white phosphorus with the amino carbenes CXY and CY′$_2$, respectively (Figure 1).[13]

We have discovered that phosphide formation of P_4 degradation with the silanides M[Si-*t*-Bu_3] (M = Na, K) and Na[SiPh-*t*-Bu_2] depends strongly on the stoichiometry and solvent.[14−19] Using the reactants in molar ratios from 1:2 to 1:4, as shown in Scheme 1, different products were formed: (i) The tri-*tert*-butylsilylated (supersilylated) tetraphosphenediides M_2[**1**] (M = Na, K) were obtained from the reaction of P_4 and M[Si-*t*-Bu_3] (M = Na, K) in a molar ratio of 1:2 in THF.[14,15] (ii) The supersilylated octaphosphides M_4[**2**] (M = Na, K), however, were also synthesized in a 1:2 stoichiometry, but in weakly polar solvents (heptane, *t*-BuOMe, etc.).[14,15] (iii) The synthesis of the supersilylated tetraphosphides M_3[**3**] (M = Li, Na) was achieved by the reaction of P_4 with the silanides M[Si-*t*-Bu_3] (M = Li, Na) in a 1:3 stoichiometry in benzene; however, in THF, the M_3[**3**] compounds (M = Li, Na) are unstable, and, thereby, (iv) M[**4**] and M_2[PSi-*t*-Bu_3] (M = Li, Na) were formed.[16] (v)

(2) (a) Wiberg, N.; Fischer, G.; Bachhuber, H. *Chem. Ber.* **1974**, *107*, 1456. (b) Wiberg, N.; Fischer, G.; Bachhuber, H. *Z. Naturforsch.* **1979**, *84b*, 1385. (c) Wiberg, N.; Fischer, G.; Bachhuber, H. *Angew. Chem., Int. Ed. Engl.* **1977**, *16*, 780.
(3) Hayon, E.; Simic, M. *J. Am. Chem. Soc.* **1972**, *94*, 42.
(4) (a) Wiberg, N.; Bayer, H.; Bachhuber, H. *Angew. Chem., Int. Ed. Engl.* **1975**, *14*, 177–178. (b) Veith, M. M.; Schlemmer, G. *Z. Anorg. Allg. Chem.* **1982**, *494*, 7.
(5) (a) Wiberg, N.; Joo, W.-Ch.; Uhlenbrock, W. *Angew. Chem.* **1968**, *80*, 661. (b) Wiberg, N.; Uhlenbrock, W. *J. Organomet. Chem.* **1974**, *70*, 239. (c) Wiberg, N.; Uhlenbrock, W. *Angew. Chem.* **1970**, *9*, 70–71. (d) Wiberg, N.; Bayer, H.; Meyers, R. *Chem. Ber.* **1979**, *112*, 2718. (e) Veith, M. *Acta Crystallogr., Sect. B* **1975**, *31*, 678.
(6) Lerner, H.-W.; Bolte, M.; Wiberg, N. *J. Organomet. Chem.* **2002**, *649*, 246.
(7) Lerner, H.-W.; Wiberg, N.; Polborn, K. *Z. Naturforsch.* **2002**, *57b*, 1199–1206.
(8) Lerner, H.-W.; Wiberg, N.; Bats, J. W. *J. Organomet. Chem.* **2005**, *690*, 3898.
(9) Lerner, H.-W.; Sänger, I.; Schödel, F.; Polborn, K.; Bolte, M.; Wagner, M. *Z. Naturforsch.* **2007**, *62b*, 1285.
(10) (a) Wiberg, N. *Coord. Chem. Rev.* **1997**, *163*, 217. (b) Wiberg, N.; Karampatses, P.; Kühnel, E.; Veith, M.; Huch, V. *Z. Anorg. Allg. Chem.* **1988**, *562*, 91.
(11) Fritz, G.; Layher, E.; Krautscheid, H.; Mayer, B.; Matern, E.; Hönle, W.; v. Schnering, H. G. *Z. Anorg. Allg. Chem* **1992**, *611*, 56.
(12) Fox, A. R.; Wright, R. J.; Rivard, E.; Power, P. P. *Angew. Chem., Int. Ed.* **2005**, *44*, 7729.
(13) (a) Masuda, J. D.; Schoeller, W. W.; Donnadieu, B.; Bertrand, G. *Angew. Chem., Int. Ed.* **2007**, *46*, 7052. (b) Masuda, J. D.; Schoeller, W. W.; Donnadieu, B.; Bertrand, G. *J. Am. Chem. Soc.* **2007**, *129*, 14180.
(14) Wiberg, N.; Wörner, A.; Karaghiosoff, K.; Fenske, D. *Chem. Ber.* **1997**, *130*, 135.
(15) Lerner, H.-W.; Bolte, M.; Karaghiosoff, K.; Wagner, M. *Organometallics* **2004**, *23*, 6073.
(16) Lerner, H.-W.; Wagner, M.; Bolte, M. *Chem. Commun.* **2003**, 990.
(17) Lerner, H.-W.; Margraf, G.; Kaufmann, L.; Bats, J. W.; Bolte, M.; Wagner, M. *Eur. J. Inorg. Chem.* **2005**, 1932.
(18) Wiberg, N.; Wörner, A.; Lerner, H.-W.; Karaghiosoff, K.; Nöth, H. *Z. Naturforsch.* **1998**, *53b*, 1004.
(19) Lerner, H.-W. *Coord. Chem. Rev.* **2005**, *249*, 781.
(20) Chan, W. T. K.; Garcia, F.; Hopkins, A. D.; Martin, L. C.; McPartlin, M.; Wright, D. S. *Angew. Chem., Int. Ed.* **2007**, *46*, 3084.
(21) Damrauer, R.; Pusede, S. E.; Staton, G. M. *Organometallics* **2008**, *27*, 3399.

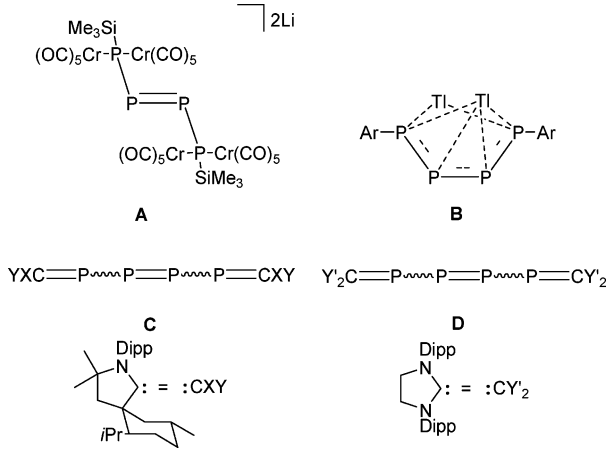

Figure 1. Derivatives of 2-tetraphosphene. Ar = C_6H_3-2,6-(C_6H_3-2,6-*i*-Pr_2)$_2$; Dipp = 2,6-*i*-$Pr_2C_6H_3$.

At last, the pentaphosphides M_2[**5**] could be synthesized by degradation of the corresponding octaphosphides M_4[**2**] with M[Si-*t*-Bu_3] (M = Na, K).[17] However, the dimeric sodium supersilylated pentaphosphide {Na_2[**5**]}$_2$ was directly accessible by treating P_4 with 4 equiv of the sodium silanide Na(thf)$_2$[Si-*t*-Bu_3] in benzene.[17]

In contrast to the reactions of P_4 with the silanides M[Si-*t*-Bu_3][19,22] (M = Li, Na) and Na[SiPh-*t*-Bu_2][19,23] in a 1:3 stoichiometry that gave the tetraphosphides M_3[**3**] (M = Li, Na) and Na_3[P_4(SiPh-*t*-Bu_2)$_3$],[16] treatment of P_4 with 3 equiv of K[Si-*t*-Bu_3] in THF first led to the formation of K_2[**1**] and K_4[**2**].[15] However, further equivalents of potassium silanide K[Si-*t*-Bu_3] caused the decomposition of the tetraphosphenediide K_2[**1**]; thereby, K[**4**] and K_2[PSi-*t*-Bu_3] were formed.[15] Therefore, the potassium tetraphosphide K_3[**3**] is yet unknown.

Very recently, we have shown that the triphosphenide Na[**4**][16,24] can be converted into Cs[**4**] by the metathesis reaction between Na[**4**] and CsF in THF (Scheme 2).[25] Transition-metal phosphanides were also available by salt metathesis. We synthesized the silver phosphanides {Ag_2[PSi-*t*-Bu_3]}$_8$[26] and {Ag_2[**5**]}$_2$[17] by reaction of AgOCN with the sodium phosphanides Na_2[PSi-*t*-Bu_3] and Na_2[**5**], respectively (Scheme 2).[17,26]

In this paper, we present the synthesis and characterization of the supersilylated alkali-metal tetraphosphenediides M_2[**1**] (M = Li, Na, Rb, Cs) and Ba[**1**]. With this selection of alkali and alkaline-earth-metal counterions, it is possible to study the tetraphosphene dianion [**1**]$^{2-}$ systematically by NMR spectroscopy. The supersilylated tetraphosphenediide also displays interesting chemical properties. Reactions of Na_2[**1**] with AuI, BH_3, $AlMe_3$, and *t*-Bu_2SnCl_2 give us the opportunity to investigate its reactivity and to decipher trends in its coordination behavior. In addition, calculations allow insight into constitutional isomerizations of tetraphosphene derivatives.

Scheme 2. Synthesis of Supersilylated Phosphides by Salt Metathesis Reaction

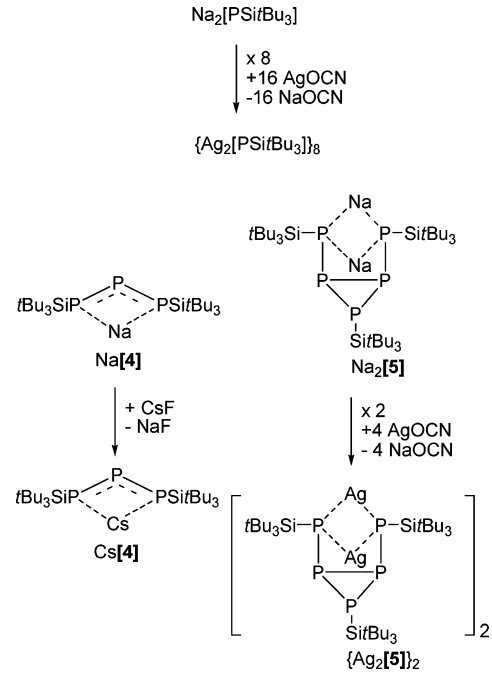

Results and Discussion

Synthesis. The lithium tetraphosphenediide Li_2[**1**] was prepared by the reaction of P_4 with the silanide Li(thf)$_3$[Si-*t*-Bu_3][9] in a molar ratio of 1:2 in THF by a synthetic route analogous to that of M_2[**1**] (M = Na, K). As we noted previously, the cesium silanide Cs[Si-*t*-Bu_3] appears to be unstable in THF at room temperature. We observed that, when *t*-Bu_3SiBr was treated with an excess of cesium metal in tetrahydrofuran at room temperature, the cesium enolate Cs[OCH=CH_2] and the supersilane *t*-Bu_3SiH formed, rather than Cs[Si-*t*-Bu_3].[25] Therefore, we decided to synthesize the tetraphosphenediides M_2[**1**] (M = Rb, Cs) and the barium derivative Ba[**1**] by the metathesis reaction between Na_2[**1**] and the corresponding metal halides in THF. NMR spectroscopy confirmed the structures of the tetraphosphenediides M_2[**1**] (M = Rb, Cs) and Ba[**1**]. Moreover, ^{31}P NMR experiments revealed that, in THF, the sodium tetraphosphenediide Na_2[**1**] possesses a cis configuration. However, treatment of Na_2[**1**] with 18-crown-6 led to the formation of the ion-separated *trans*-tetraphosphenediide [Na(18-crown-6)(thf)$_2$]$_2$[**1**]. The tetraphosphenediide [Na(18-crown-6)-(thf)$_2$]$_2$[**1**] was analyzed using X-ray crystallography. In contrast to [Na(18-crown-6)(thf)$_2$]$_2$[**1**], the structure of thallium tetraphosphenediide **B** reveals a planar dianionic tetraphosphene core with a cis configuration that is complexed to Tl ions disposed equidistant above and below the P_4array.

On the one hand, metal exchange reactions can easily be carried out between Na_2[**1**] and alkali-metal halides, as well

(22) Wiberg, N.; Amelunxen, K.; Lerner, H.-W.; Schuster, H.; Nöth, H.; Krossing, I.; Schmidt-Ameluxen, M.; Seifert, T. *J. Organomet. Chem.* **1997**, *524*, 1.
(23) (a) Lerner, H.-W.; Scholz, S.; Bolte, M.; Wagner, M. *Z. Anorg. Allg. Chem.* **2004**, *630*, 443. (b) Lerner, H.-W.; Scholz, S.; Bolte, M. *Z. Anorg. Allg. Chem.* **2001**, *627*, 1638.
(24) Wiberg, N.; Wörner, A.; Lerner, H.-W.; Karaghiosoff, K.; Fenske, D.; Baum, G.; Dransfeld, A.; Schleyer, P. v. R. *Eur. J. Inorg. Chem.* **1998**, 833.
(25) Lerner, H.-W.; Sänger, I.; Schödel, F.; Lorbach, A.; Bolte, M.; Wagner, M. *Dalton Trans.* **2008**, 787.
(26) Lerner, H.-W.; Margraf, G.; Bats, J.; Wagner, M. *Chem. Commun.* **2005**, 4545.

Scheme 3. Synthesis of Cyclotetraphosphane **6** by Reaction of $Na_2[t\text{-}Bu_3SiPPPPSi\text{-}t\text{-}Bu_3]$ with AuI

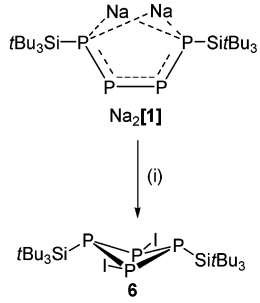

(i) +2 AuI, –2 "NaAu", in THF at room temperature.

as BaI_2, and on the other hand, the addition of AuI to tetraphosphenediide $Na_2[\mathbf{1}]$ surprisingly yielded 1,3-diiodo-2,4-disupersilyl-cyclotetraphosphane **6**, which can be considered as an isomer of disupersilylated diiodotetraphosphene, as shown in Scheme 3. This reaction occurs quantitatively, as determined by ^{31}P NMR spectroscopy, with the signals of the tetraphosphenediide $Na_2[\mathbf{1}]$ ^{31}P nuclei disappearing completely.

Reactivity. The alkali-metal tetraphosphenediides $M_2[\mathbf{1}]$ (M = Li, Na, K, Rb, Cs) and Ba[**1**] are sensitive to protonolysis. Competitive protonolysis of supersilylated sodium phosphides reveals the following basicity: Na[**4**] < $Na_2[\mathbf{1}]$ < $Na_4[\mathbf{2}]$ ~ $Na_3[\mathbf{3}]$ ~ $Na_2[\mathbf{5}]$ ~ Na[PHSi-*t*-Bu_3] < Na_2[PSi-*t*-Bu_3]. When treated with an excess of trifluoroacetic acid in C_6D_6, the tetraphosphenediides are converted into supersilyl phosphane *t*-Bu_3SiPH_2[27] and, up to now, not exactly identified polyphosphanes. However, treatment of the sodium tetraphosphenediide $Na_2[\mathbf{1}]$ with the Lewis acids BH_3 and $AlMe_3$ gives more insight into the reaction behavior of $Na_2[\mathbf{1}]$ toward electrophiles than its protonolysis. At first, the reaction of $Na_2[\mathbf{1}]$ with BH_3 and $AlMe_3$ led to the formation of the corresponding complexes $\mathbf{7}(BH_3)_2$ and $\mathbf{7}(AlMe_3)_2$, respectively, as determined by mass spectrometry and ^{31}P NMR spectroscopy. Obviously, at temperatures higher than −50 °C, the adduct $\mathbf{7}(BH_3)_2$ was transformed into **8**, as shown in Scheme 4. The coupling constants of **8** and the contact-ion pair $Na_2[\mathbf{1}]$ have nearly the same values (Figure 4). The ^{11}B NMR spectrum of the reaction between $Na_2[\mathbf{1}]$ and BH_3 shows a broad signal that can be assigned to **8** and a signal with a quintet pattern. The quintet signal reveals a chemical shift, as well as BH coupling constants that are characteristic for $Na[BH_4]$. In addition, compound **8** consists apparently of a BP_4 ring with a bridging BH_2 unit, as shown in Scheme 4.

It is interesting to note that reaction products $\mathbf{7}(AlMe_3)_2$ and **8** are thermolabile compounds. After 2 days at room temperature, in the ^{31}P NMR spectrum of the reaction between $Na_2[\mathbf{1}]$ and BH_3, we observed several new resonances in the range of saturated P atoms, whereas the signals of "unsaturated" P nuclei from **8** have disappeared (e.g., (*t*-$Bu_3Si)_3P_7$,[28] (*t*-$Bu_3Si)_2P_4$[29]). The thermolysis reaction of $\mathbf{7}(AlMe_3)_2$ occurs quantitatively after 1 week, as determined by ^{31}P NMR spectroscopy, with the signals of $\mathbf{7}(AlMe_3)_2$ disappearing completely. The chemical shifts in the ^{31}P NMR spectrum are in the range of polyphosphanes; however, we could identify only a few products herein (e.g., *t*-$Bu_3SiPHMe$, *t*-Bu_3SiPMe_2). Treatment of $Na_2[\mathbf{1}]$ with *t*-Bu_2SnCl_2 led to the formation of the phosphanylcyclotriphosphane **9**, a further constitutional isomer of the supersilylated tetraphosphene (Scheme 5). In contrast to analogous nitrogen compounds that consist of N_4 chains in cis or trans configuration, neutral 2-tetraphosphenes of the type *t*-$Bu_3SiRP{-}P{=}P{-}PR'Si\text{-}t\text{-}Bu_3$, with covalent RP and R′P bonds, seem to be less stable. On the one hand, tetraphosphenes *t*-$Bu_3SiRP{-}P{=}P{-}PR'Si\text{-}t\text{-}Bu_3$ with bulky R and R′ substituents undergo isomerization reactions with the formation of isolable phosphanylcyclotriphosphane and cyclotetraphosphane derivatives (e.g., **9** (R = R′ = *t*-Bu_2Sn), **6** (R = I, R′ = I), Schemes 3 and 5), and on the other hand, decomposition of the protonated disupersilylated *cis*- and *trans*-tetraphosphene (R = H, R′ = H) occurs in the formation of *t*-Bu_3SiPH_2. In this context, it is interesting to note that the decomposition of *cis*- and *trans*-tetraphosphenes *t*-$Bu_3SiHP{-}P{=}P{-}PHSi\text{-}t\text{-}Bu_3$ looks very similar to tetrazene degradation.

The alkali-metal tetraphosphenediides $M_2[\mathbf{1}]$ (M = Li, Na, K, Rb, Cs) and Ba[**1**] can easily be oxidized. Generally, treatment of $M_2[\mathbf{1}]$ (M = Li, Na, K, Rb, Cs) and Ba[**1**] with TCNE gives the bicyclo[1.1.0]tetraphosphane (*t*-$Bu_3Si)_2P_4$.[29] This oxidation is accompanied by a color change from red-purple to pale yellow.

The oxidation to the bicyclo[1.1.0]tetraphosphane (*t*-$Bu_3Si)_2P_4$ can, however, be reversed by reduction with sodium.[29] When the bicyclo[1.1.0]tetraphosphane (*t*-$Bu_3Si)_2P_4$ is exposed to an excess of sodium metal at room temperature, the dark purple color appears and the NMR signals corresponding to the tetraphosphene dianion are observed.

In weakly polar solvents, the tetraphosphenediides $M_2[\mathbf{1}]$ (M = Li, Rb, Cs) and Ba[**1**] dimerize to $M_4[\mathbf{2}]$ (M = Li, Rb, Cs) and $Ba_2[\mathbf{2}]$, as the tetraphosphenediides $M_2[\mathbf{1}]$ (M = Na, K) do (Scheme 1). In summary, the related $M_2[\mathbf{1}]$ (M = Li, Rb, Cs) and Ba[**1**] possess nearly the same chemical properties as we have found for $M_2[\mathbf{1}]$ (M = Na, K).[14,15,30]

NMR Spectra. When considering the ^{29}Si and ^{31}P NMR spectra of the alkali-metal tetraphosphenediides $M_2[\mathbf{1}]$ (M = Li, Na, K, Rb, Cs) and Ba[**1**], no certain general trends can be observed. However, the NMR spectra of $M_2[\mathbf{1}]$ (M = Li, Rb, Cs) and Ba[**1**] resemble those of the sodium and potassium tetraphosphenediides $M_2[\mathbf{1}]$ (M = Na, K).[15,16] The $^{31}P\{^1H\}$ NMR spectra of the alkali and alkaline-earth-metal tetraphosphenediides show multiplets with the splitting pattern of an AA′XX′ spin system. The signals of the

(27) Alternative synthesis of *t*-Bu_3SiPH_2 was achieved by the reaction of *t*-$Bu_3SiO_3SCF_3$ with $LiPH_2$. Wiberg, N.; Schuster, H. *Chem. Ber.* **1991**, *124*, 93.

(28) Kovács, I.; Baum, G.; Fritz, G.; Fenske, D.; Wiberg, N.; Schuster, H.; Karaghiosoff, K. *Z. Anorg. Allg. Chem.* **1993**, *619*, 453.

(29) Wiberg, N.; Wörner, A.; Lerner, H.-W.; Karaghiosoff, K. *Z. Naturforsch.* **2002**, *57b*, 1027.

(30) (a) Sänger, I.; Schödel, F.; Bolte, M.; Wagner, M.; Lerner, H.-W. Unpublished work. (b) Wörner, A. Ph.D. Thesis, University of Munich, Munich, Germany, 1998.

Scheme 4. Reaction of $Na_2[t\text{-}Bu_3SiPPPPSi\text{-}t\text{-}Bu_3]$ with BH_3 and $AlMe_3$

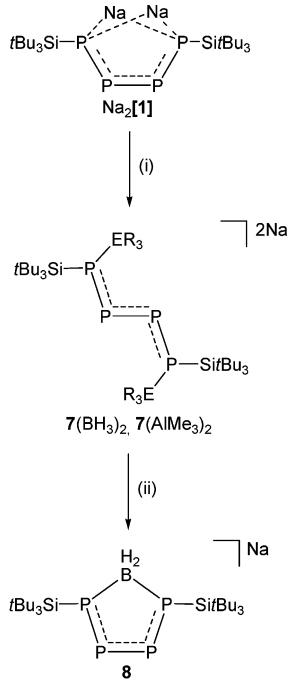

(i) +2 ER_3 , $ER_3 = BH_3$ in THF at -80°C; $ER_3 = AlMe_3$ in THF at -78°C; (ii) $Na[BH_4]$, $ER_3 = BH_3$.

Scheme 5. Synthesis of Phosphanylcyclotriphospane **9**

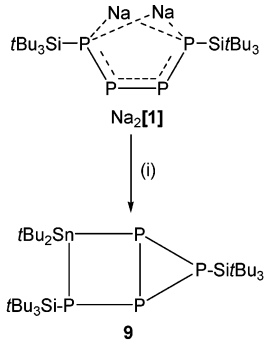

(i) + $t Bu_2SnCl_2$, –2NaCl, in THF at room temperature.

"unsaturated" P atoms tend to be shifted downfield in tetraphosphenediides containing the heavier alkali-metal atoms, with the exception of Cs, but the change in chemical shift is small, making such trends more difficult to discern (Figure 2). In addition, the signals of the phosphorus nuclei P(2) and P(3) are shifted downfield as the metal is changed from Cs to Ba. The ^{31}P shifts of P(1) and P(4) of M_2[**1**] (M = Li, Na, K, Rb, Cs) and Ba[**1**] range from $\delta = -52.9$ to 19.0. As shown in Figure 2, the signals of the P(2) and P(3) nuclei of the tetraphosphenediides M_2[**1**] (M = Rb, Cs) and Ba[**1**] are broadened, as well as those for P(1) and P(4), due to the coupling of P(1) and P(4) with Rb, Cs, and Ba, respectively, whereas the spectrum of the contact-ion pair Na_2[**1**] shows only a relative broad signal for the phosphidic P atoms P(1) and P(4). This can be explained by the fact that in M_2[**1**] (M = Rb, Cs) and Ba[**1**], the larger cations Rb^+, Cs^+, and Ba^{2+} are coordinated to all P atoms of the disupersilylated tetraphosphene dianion, whereas the Na^+ cations of Na_2[**1**] are only in contact with P(1) and P(4). In contrast to ^{31}P NMR spectra of the tetraphosphene derivatives **C** and **D** that reveal two sets of signals, suggesting an equilibrium of *cis*- and *trans*-tetraphosphene isomers in solution, we found in the ^{31}P NMR spectrum of the ion-separated tetraphosphenediide $[Na(18\text{-crown-}6)(thf)_2]_2$[**1**], as well as in that of the contact-ion pair Na_2[**1**], only one set of signals.

Further information about the bonding situation in alkali-metal tetraphosphenediides M_2[**1**] (M = Li, Na, K, Rb, Cs) and Ba[**1**] may be obtained from the PP coupling constants. It is interesting to note that the ^{31}P NMR spectra of the ion-

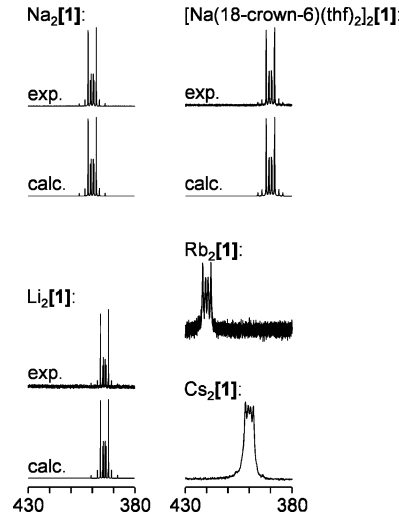

Figure 2. Observed and calculated ^{31}P NMR spectra of $[Na(18\text{-crown-}6)(thf)_2]_2$[**1**] and M_2[**1**] (M = Li, Na, Rb, Cs). Signals of the "unsaturated" nuclei P(2) and P(3) of $[t\text{-}Bu_3SiP(1)P(2)P(3)P(4)Si\text{-}t\text{-}Bu_3]^{2-}$ are drawn. Chemical shifts and coupling constants [Hz] of tetraphosphenediides. Li_2[**1**]: δ 394.2, −52.9, $^1J_{P(2)P(3)} = -500.5$, $^1J_{P(1)P(2)} = -426.2$, $^2J_{P(1)P(3)} = -29.8$, $^3J_{P(1)P(4)} = 198.3$. Rb_2[**1**]: δ 419.9, −35.4. Cs_2[**1**]: δ 400.1, −44.4.

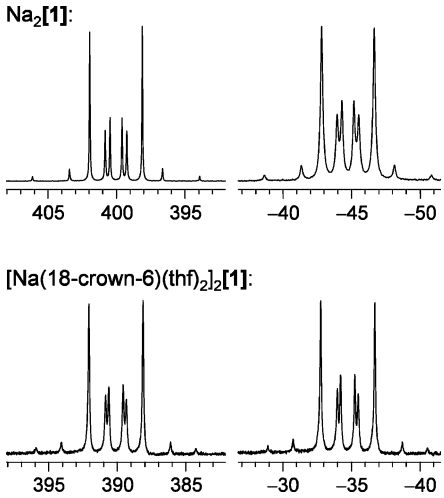

Figure 3. A comparison of the ^{31}P NMR spectra of [Na(18-crown-6)(thf)$_2$]$_2$[**1**] and the contact-ion pair Na$_2$[**1**]. Chemical shifts and coupling constants [Hz] of [Na(18-crown-6)(thf)$_2$]$_2$[**1**]: δ 390.1, −34.7, $^1J_{P(2)P(3)}$ = −518.7, $^1J_{P(1)P(2)}$ = −451.8, $^2J_{P(1)P(3)}$ = −28.7, $^3J_{P(1)P(4)}$ = 126.7. Chemical shifts and coupling constants [Hz] of Na$_2$[**1**]: δ 400.0, −45.2, $^1J_{P(2)P(3)}$ = −502.1, $^1J_{P(1)P(2)}$ = −432.3, $^2J_{P(1)P(3)}$ = −34.2, $^3J_{P(1)P(4)}$ = 185.4.

separated tetraphosphenediide [Na(18-crown-6)(thf)$_2$]$_2$[**1**] and of the contact-ion pair Na$_2$[**1**] reveal different coupling constants. As listed in the caption of Figure 3, the values of coupling constants $^1J_{P(2)P(3)}$ and $^1J_{P(1)P(2)}$ of [Na(18-crown-6)(thf)$_2$]$_2$[**1**] are significantly higher than those of the contact-ion pair Na$_2$[**1**], but the values of both tetraphosphenediides lie in the double bond region. Due to through-space coupling and s-cis/s-trans isomerization, the value of the constant $^3J_{P(1)P(4)}$ of [Na(18-crown-6)(thf)$_2$]$_2$[**1**] is remarkably large. This predicts a bonding situation as found in 1,3-butadiene. However, the increase in the $^3J_{P(1)P(4)}$ coupling constants going from [Na(18-crown-6)(thf)$_2$]$_2$[**1**] to the contact-ion pair Na$_2$[**1**] is significant and is presumably caused by a different s-cis-/s-trans rotamer relation of the contact-ion pair Na$_2$[**1**] and [Na(18-crown-6)(thf)$_2$]$_2$[**1**]. Generally, the trend of the coupling constant values of alkali-metal tetraphosphenediides M$_2$[**1**] (M = Li, Na, K) is comparable with the tendency of the CC coupling constants of 1,3-butadiene (H$_2$C(1)═C(2)H−HC(3)═C(4)H$_2$: $^1J_{C(2)C(3)}$ = 53.7 Hz, $^1J_{C(1)C(2)}$ = 68.8 Hz, $^2J_{C(1)C(3)}$ = <1 Hz, $^3J_{C(1)C(4)}$ = 9.1 Hz).[31] In contrast to the apparent constants of alkali-metal tetraphosphenediides M$_2$[**1**] (M = Li, Na, K), the $^3J_{P(1)P(4)}$ value of the tetraphosphene **A** was less than 1 Hz. This result is in correlation with the molecular structure of tetraphosphene derivatives. Large $^3J_{P(1)P(4)}$ values suggest the existence of s-cis rotamers or cis isomers, whereas small coupling constants correlate with a trans configuration of tetraphosphene derivatives. Therefore, $^3J_{P(1)P(4)}$ coupling constants are valuable diagnostic tools for an assessment of s-cis/s-trans isomerization of P$_4$ chains.

On the one hand, the coupling constants of the product of the reaction between Na$_2$[**1**] and BH$_3$ (**8**) and the contact-ion pair Na$_2$[**1**] possess nearly the same values (e.g., Na$_2$[**1**]: $^3J_{P(1)P(4)}$ = 185.4 Hz. **8**: $^3J_{P(1)P(4)}$ = 188.9 Hz. Na$_2$[**1**]: $^1J_{P(2)P(3)}$ = −502.1 Hz. **8**: $^1J_{P(2)P(3)}$ = −507.0 Hz), and on the other hand, the ^{31}P NMR spectrum of the AlMe$_3$ complex **7**(AlMe$_3$)$_2$ reveals coupling constants that are similar to those of [Na(18-crown-6)(thf)$_2$]$_2$[**1**] (Figure 5). Therefore, in solution, a cis configuration of **8** seems to be presumable. Due to the coupling of Al with the P(1) and P(4) nuclei, the signal of P(1) and P(4) was not observable in the ^{31}P NMR spectrum of **7**(AlMe$_3$)$_2$. As depicted in Figure 4, the ^{31}P NMR spectrum of the reaction mixture of Na$_2$[**1**] and BH$_3$ at −80 °C shows only signals that can be assigned to the starting material Na$_2$[**1**], suggesting no adduct formation at this temperature. As expected, the signals of **8** are broad, due to BP coupling, as revealed in the ^{31}P NMR spectrum of the reaction between Na$_2$[**1**] and BH$_3$.

The ^{29}Si NMR spectra of the contact-ion pair Na$_2$[**1**] and [Na(18-crown-6)(thf)$_2$]$_2$[**1**], as well as of M$_2$[**1**] (M = Li, Na, K, Rb, Cs) and Ba[**1**], resemble each another. Due to the large coupling constants between P(2)P(3) and P(1)P(4), the ^{29}Si NMR spectrum of [Na(18-crown-6)(thf)$_2$]$_2$[**1**] consists of a deceptively simple triplet of triplet pattern of an

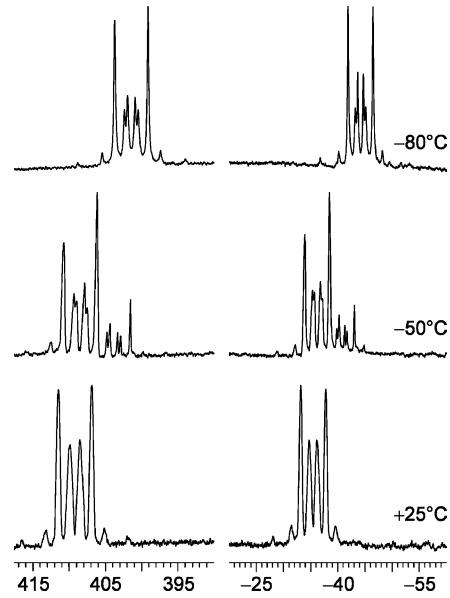

Figure 4. ^{31}P NMR spectra of the reaction of Na$_2$[**1**] with BH$_3$. Chemical shifts and coupling constants [Hz] of **8**: δ 409.7, −35.0, $^1J_{P(2)P(3)}$ = −507.0, $^1J_{P(1)P(2)}$ = −429.9, $^2J_{P(1)P(3)}$ = −35.4, $^3J_{P(1)P(4)}$ = 188.9.

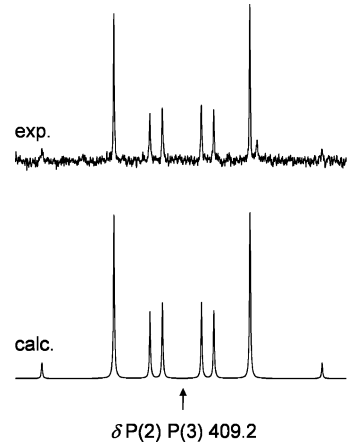

Figure 5. ^{31}P NMR spectrum of the adduct of Na$_2$[**1**] with AlMe$_3$. Chemical shifts and coupling constants [Hz] of **7**(AlMe$_3$)$_2$: δ 409.2, $^1J_{P(2)P(3)}$ = −509.8, $^1J_{P(1)P(2)}$ = −434.3, $^2J_{P(1)P(3)}$ = −3.7, $^3J_{P(1)P(4)}$ = 162.4.

(31) Becher, G.; Lüttke, W.; Schrumpf, G. *Angew. Chem., Int. Ed. Engl.* **1973**, *12*, 339–340.

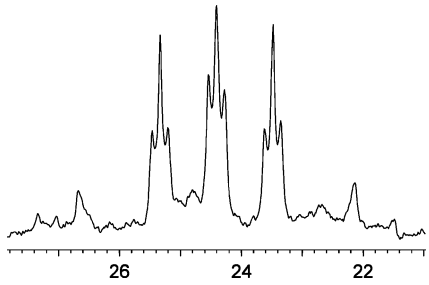

Figure 6. ^{29}Si NMR spectrum of [Na(18-crown-6)(thf)$_2$]$_2$[**1**]. Chemical shifts and coupling constants [Hz] of [Na(18-crown-6)(thf)$_2$]$_2$[**1**]: δ 24.2, $^1J_{SiP} + {}^4J_{SiP} = 46.0$, $^2J_{SiP} + {}^3J_{SiP} = 6.5$.

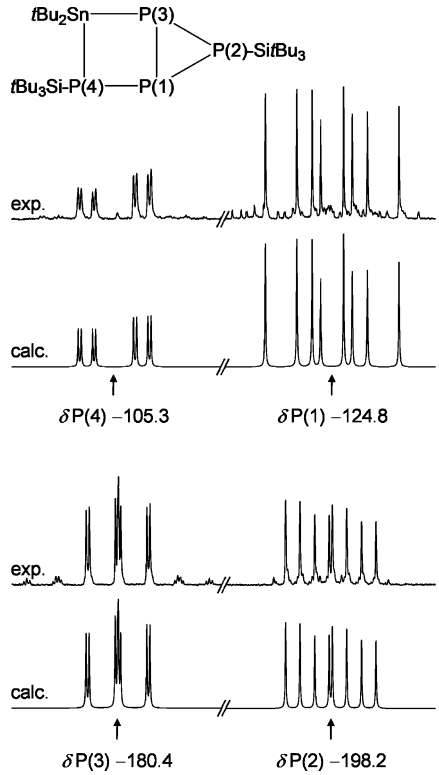

Figure 7. ^{31}P{^{1}H} NMR spectrum of the phosphanylcyclotriphosphane **9**. Chemical shifts and coupling constants [Hz] of **9** (C_6D_6, external TMS): δ −105.3 (m, $^1J_{P(1)P(4)} = -280.2$, $^2J_{P(2)P(4)} = 74.6$, $^2J_{P(3)P(4)} = 16.8$, P(4)), −124.8 (m, $^1J_{P(1)P(2)} = -238.7$, $^1J_{P(1)P(3)} = -160.4$, P(1)), −180.4 (m, $^1J_{P(2)P(3)} = -147.9$, P(3)), −198.2 (m, P(2)).

AA′MM′X spin system, as shown in Figure 6. The relative difference in chemical shift of supersilylated tetraphosphenediides M$_2$[**1**] (M = Li, Na, K, Rb, Cs) and Ba[**1**] is generally small, and it is always more pronounced for the ^{31}P signals than for the ^{29}Si signals. In addition, no general trend can be applied to the relative shifts of the ^{29}Si nuclei of M$_2$[**1**] (M = Li, Na, K, Rb, Cs) and Ba[**1**].

The ^{31}P{^{1}H} NMR spectrum of cyclotetraphosphane **6** reveals two triplets with the splitting pattern of an A_2X_2 spin system and a coupling constant value of $^1J_{PP} = 226.7$ Hz. The signals of P nuclei of **6** appear at low field in the typical range of P_4-ring compounds (δ 149.0 (PI), −34.9 (PSi-*t*-Bu$_3$)). As shown in Figure 7, the chemical shifts of the phosphorus nuclei of the phosphanylcyclotriphosphane **9**, however, appear at high field (δP(1) −124.8, δP(2) −198.2, δP(3) −180.4, δP(4) −105.3), as was found for δ in 2,4,5-tris(supersilyl)bicyclo[2.1.0^{1,3}]pentaphosphane.[17,18] The presence of a cyclotriphosphane ring in **9** is indicated by the chemical shift of P(1), P(2), and P(3), as well as by the large and negative coupling constants ($^1J_{P(1)P(2)} = -238.7$ Hz, $^1J_{P(1)P(3)} = -160.4$ Hz, $^1J_{P(2)P(3)} = -147.9$ Hz). The direct connection of the P(1) and P(4) center is indicated by the large and negative coupling constant between P(1) and P(4) ($^1J_{P(1)P(4)} = -280.2$ Hz). The neighborhood of the Sn atom causes large and positive coupling constants ($^1J_{119SnP(4)} = 946.0$ Hz, $^1J_{117SnP(4)} = 905.0$ Hz, $^1J_{119SnP(3)} = 628.8$ Hz, $^1J_{117SnP(3)} = 600.6$ Hz) between P(3), as well as P(4) and ^{117}Sn and ^{119}Sn, respectively. The resulting PP, ^{117}SnP, and ^{119}SnP coupling constants and ^{31}P chemical shifts are summarized in the Experimental Section and the Figure 7 caption.

Crystal Structures. The molecular structures of the tetraphosphenediide [Na(18-crown-6)(thf)$_2$]$_2$[**1**] and cyclotetraphosphane **6** are shown in Figures 8 and 9 and Figures S1 and S2 in the Supporting Information. Selected bond lengths and angles are listed in the corresponding figure captions and Table 1. Crystal data and refinement details are given in Table 2.

Figure 8 represents the molecular structure of the tetraphosphenediide [Na(18-crown-6)(thf)$_2$]$_2$[**1**] (monoclinic, $P2_1/n$; for selected bond lengths and angles, see Table 1 and Figure 8 caption). The disodium *trans*-tetraphosphenediide crystallizes with a half-molecule of [Na(18-crown-6)(thf)$_2$]$_2$[**1**] and a half-molecule of 18-crown-6 in the asymmetric unit (Figure S1 in the Supporting Information). In contrast to the thallium tetraphosphenediide **B**, the ion-separated sodium tetraphosphenediide [Na(18-crown-6)(thf)$_2$]$_2$[**1**] possesses a trans configuration, as found in the structure of the lithium complex **A**.[11] The molecular structure of the tetraphosphenediide [Na(18-crown-6)(thf)$_2$]$_2$[**1**] shows three short PP bonds, one of 2.126(9) Å and two of 2.133(6) Å, and an almost planar SiPPPPSi skeleton. The PP distances in [Na(18-crown-6)(thf)$_2$]$_2$[**1**] are between PP single and PP double bonds, comparable with those found in the structures of the tetraphosphene derivative **B**[12] (Table 1) and, therefore, longer than PP double bonds found in the structures of tetraphosphenes **A**[11] and **C**,[13] as well as the PP bonds in the structures of triphosphenides M[**4**] (M = Na, K, Cs) (average PP bond lengths in M[**4**]: 2.096(20) Å (Na), 2.072(2) Å (K), 2.090(3) Å (Cs)).[15,24,25] It is interesting to note that the structure of the tetraphosphene **A** features one short double bond (2.025(3) Å) in the range of diphosphenes[29] and two PP single bonds (2.219(3) Å).[11] The structure of tetraphosphene **C** reveals shorter PP single bonds compared to those in **A** and a significantly longer double bond than in **A**.[13] On the one hand, the PP distances (2.126(9) and 2.133(6) Å) in [Na(18-crown-6)(thf)$_2$]$_2$[**1**] are somewhat longer than those found in diphosphenes[32] and the triphosphenides M[**4**] (M = Na, K, Cs),[15,24,25] and on the other hand, the PP bonds in [Na(18-crown-6)(thf)$_2$]$_2$[**1**] are nearly identical and have lengths shorter than the PP single bonds in polyphosphanes.[32] These findings suggest a π system in [Na(18-crown-

(32) (a) *Cambridge Structural Database (CSD)*, version 5.29; with three updates, January 2008; Allen, 2002. (b) Allen, F. H. *Acta Crystallogr.* **2002**, *B58*, 380.

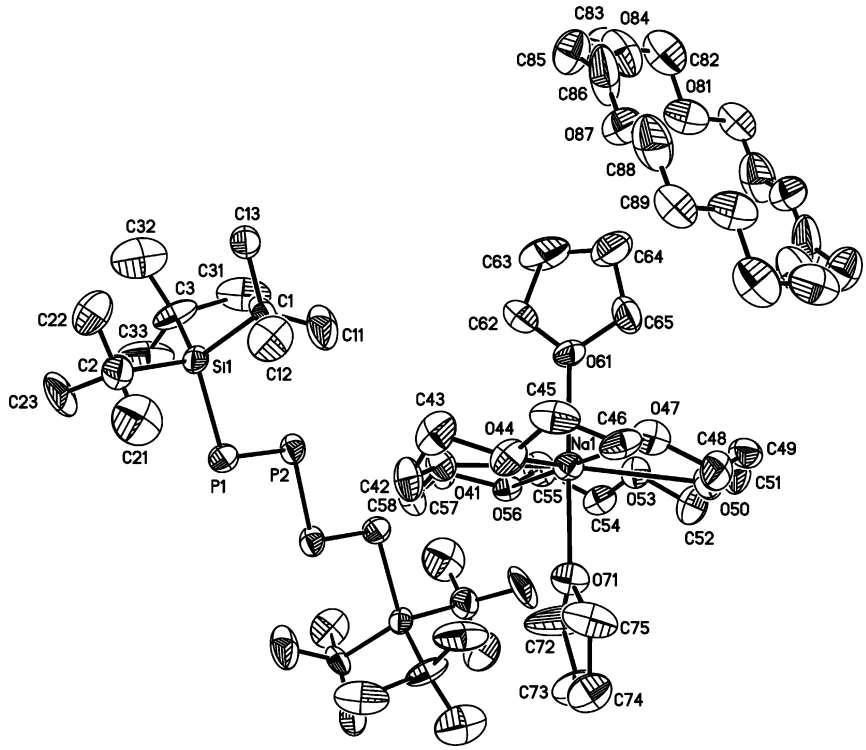

Figure 8. Solid-state structure of [Na(18-crown-6)(thf)$_2$]$_2$[**1**] and one molecule of 18-crown-6. Displacement ellipsoids are drawn at the 20% probability level. Hydrogen atoms have been omitted for clarity. Selected bond lengths (Å) and angles (deg): Si(1)−C(1) = 1.984(16), Si(1)−C(2) = 2.07(3), Si(1)−P(1) = 2.213(6), P(1)−P(2) = 2.133(6), P(2)−P(2)#1 = 2.126(9), Na(1)−O(71) = 2.304(13), Na(1)−O(61) = 2.341(11), Na(1)−O(41) = 2.611(12), Na(1)−O(56) = 2.642(10), Na(1)−O(44) = 2.739(12), Na(1)−O(47) = 2.789(12), Na(1)−O(50) = 2.870(12), Na(1)−O(53) = 2.914(10), C(3)−Si(1)−C(1) = 108.1(10), C(3)−Si(1)−C(2) = 113.4(12), C(1)−Si(1)−C(2) = 107.7(9), C(3)−Si(1)−P(1) = 115.8(6), C(1)−Si(1)−P(1) = 111.7(6), C(2)−Si(1)−P(1) = 99.8(7), P(2)−P(1)−Si(1) = 103.0(3), P(2)#1−P(2)−P(1) = 100.4(3). Symmetry transformations used to generate equivalent atoms: #1 $-x+1$, $-y$, $-z+1$; #2 $-x+1$, $-y+1$, $-z+1$.

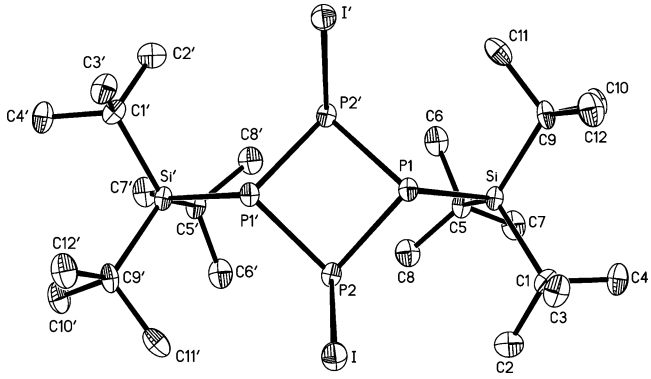

Figure 9. Solid-state structure of **6**. Thermal ellipsoids are drawn at the 50% probability level. Hydrogen atoms have been omitted for clarity. Selected bond lengths (Å) and angles (deg): I−P(2) = 2.5126(12), P(1)−P(2) = 2.214(3), P(1)−P(2)#1 = 2.214(3), P(1)−Si = 2.3171(15), Si−C(9) = 1.931(9), Si−C(5) = 1.941(4), Si−C(1) = 1.958(8), P(2)−P(1)#1 = 2.214(3), P(2)−P(1)−P(2)#1 = 87.49(7), P(2)−P(1)−Si = 108.94(10), P(2)#1−P(1)−Si = 112.58(10), C(9)−Si−C(5) = 113.1(4), C(9)−Si−C(1) = 112.6(2), C(5)−Si−C(1) = 111.9(4), C(9)−Si−P(1) = 100.8(2), C(5)−Si−P(1) = 115.33(14), C(1)−Si−P(1) = 102.2(2), P(1)−P(2)−P(1)#1 = 84.81(6), P(1)−P(2)−I = 101.69(7), P(1)#1−P(2)−I = 101.76(7) Symmetry transformations used to generate equivalent atoms: #1 $-x$, y, $-z+1/2$.

6)(thf)$_2$]$_2$[**1**] analogous to that in **B**. In addition, the PP bonds in [Na(18-crown-6)(thf)$_2$]$_2$[**1**] conform formally to a bond order of 1.33, whereas the PP bond length in triphosphenides M[**4**] (M = Na, K, Cs) formally gives a PP bond order of 1.5. The distance for P−Si-*t*-Bu$_3$ of 2.213(6) Å in [Na(18-crown-6)(thf)$_2$]$_2$[**1**] is of a characteristic length for PSi bonds in supersilylated phosphides (mean length of PSi bonds = 2.251 Å).[14−19,24−26,32] The supersilylated sodium tetraphosphenediide [Na(18-crown-6)(thf)$_2$]$_2$[**1**] displays a PPP angle of 100.4(3)°. As depicted in Figure S1 in the Supporting Information, the structure of [Na(18-crown-6)(thf)$_2$]$_2$[**1**] features long PNa distances (shortest PNa distance = 7.065 Å), suggesting no interaction between the sodium cations and the P atoms of the tetraphosphene dianions. Apparently, in [Na(18-crown-6)(thf)$_2$]$_2$[**1**], the negative charge of the dianion is distributed over the whole P_4 chain, suggesting a decrease of nucleophilicity of P centers of [**1**]$^{2-}$, compared to that of related supersilylated phosphanides. As shown in Figure 8, the sodium cations in [Na(18-crown-6)(thf)$_2$]$_2$[**1**] are coordinated by eight O atoms of two THF molecules and one 18-crown-6 molecule in a hexagonal bipyramidal fashion.

Table 1. Selected Bond Lengths [Å] and Angles [°] for 2-Tetraphosphenes $R_2P-P=P-PR_2$

	P−P	P=P	P−P−P
[Na(18-crown-6)(thf)$_2$]$_2$[**1**] (*trans*)	2.133(6)	2.126(9)	100.4(3)
10 *trans*-[HP−P=P−PH]$^{2-a}$	2.176	2.098	108.0
11 *cis*-[HP−P=P−PH]$^{2-a}$	2.158	2.090	115.3
14 *trans*-[H_3SiP−P=P−PSiH_3]$^{2-a}$	2.176	2.090	104.9
15 *cis*-[H_3SiP−P=P−PSiH_3]$^{2-a}$	2.162	2.085	112.7
19 *cis*-(H_3Si)NaP−P=P−PNa(SiH_3)^a	2.173	2.106	109.70
22 *trans*-H_2P−P=P−PH_2^{a}	2.250	2.048	101.14
26 *trans*-(H_3Si)HP−P=P−PH(SiH_3)^a	2.210	2.054	98.70
A[11] (*trans*)	2.219(2)	2.025(3)	105.9(1)
B[12] (*cis*)	2.143(6)	2.136(4)	101.8(1)
C[13] (*trans*)	2.191(5)	2.083(4)	92.9(2)av

^{a} Calculated at MP2/6-31G(d) as part of G3.

Table 2. Crystal Data and Structure Refinement Parameters for $[Na(18\text{-crown-}6)(thf)_2]_2$[**1**] and **6**

	$[Na(18\text{-crown-}6)(thf)_2]_2$ [**1**]·(18-crown-6)	**6**
empirical formula	$C_{76}H_{158}Na_2O_{22}Si_2$	$C_{24}H_{54}I_2P_4Si_2$
color	dark violet	yellow
shape	plate	plate
fw	1650.06	776.53
crystal system	monoclinic	monoclinic
space group	$P2_1/n$	$C2/c$
a, Å	16.006(2)	15.226(5)
b, Å	23.823(3)	8.4316(8)
c, Å	16.436(2))	26.135(8)
β, deg	115.699(10)	90.40(3)
volume, Å^3	5647.3(12)	3355.1(15)
Z	2	4
density$_{calcd}$, Mg/m^3	0.970	1.537
abs coeff μ(Mo Kα), mm^{-1}	0.148	2.150
F(000)	1800	1568
crystal size, mm^3	0.32 × 0.24 × 0.09	0.39 × 0.20 × 0.12
θ-range, deg	2.19 to 25.08	0.78 to 32.24
index ranges	$-19 \le h \le 18$ $-28 \le k \le 28$ $-19 \le l \le 19$	$-19 \le h \le 22$ $-12 \le k \le 12$ $-39 \le l \le 33$
no. of reflections collected	40 944	28 691
no. of independent reflections	9929	5333
R(int)	0.1731	0.0951
T_{min}, T_{max}	0.9542, 0.9868	0.698, 1.000
no. of data/restraints/parameter	9929/234/478	5333/0/156
goodness of fit on F^2	1.361	1.037
final R indices [$I > 2\sigma(I)$], R1, wR2	0.2468, 0.5331	0.0514, 0.1154
R indices (all data), R1, wR2	0.3635, 0.5762	0.0740, 0.1237
peak/hole, e Å^{-3}	0.936 and −0.522	2.196 and −2.057

X-ray quality crystals of **6** were grown from toluene. The phosphane **6** represents the second structurally characterized halogenated cyclotetraphosphane, but the first one with two halogen substituents on the P_4 ring. The cyclotetraphosphane **6** crystallizes in the monoclinic space group $C2/c$. The four-membered ring in **6** is puckered with PPPP torsion angles of +29.1 and −29.1°. The PP distance of 2.214(3) Å between the P atoms of the P_4 ring is in good agreement with PP distances in other cyclotetraphosphane structures.[32] The Si and I substituents are in pseudo-equatorial positions. The P−Si-*t*-Bu$_3$ bond distance of 2.317(2) Å is, on the one hand, longer than the PSi distance of 2.253 Å in the diamino(bistrimethylsilyl)cyclotetraphosphane derivative,[33] and on the other hand, it is comparable to those found in supersilylated phosphorus compounds.[15−19,24−26,32] The PI distance of 2.513(1) Å is comparable to values of 2.48−2.49 Å found for related P−I bonds.[32] The shortest intramolecular HH distance across the tetraphosphane ring is 2.13 Å, whereas the shortest intramolecular HH distances within the supersilyl groups are between 2.17 and 2.20 Å. The shortest intermolecular contact is a CH···I interaction with a HI distance of 3.30 Å, which is about 0.1 Å longer than the van der Waals contact distance.

Calculations. The experimental studies described thus far were augmented by accurate quantum chemical calculations at the G3 level on relative isomer stabilities of small molecular models containing the key structural features of tetraphosphene derivatives. Figures 11−15 illustrate the results of calculations concerning structures and relative energies of isomers of the bare dianion $[H_2P_4]^{2-}$, the disilylated dianion $[(H_3Si)_2P_4]^{2-}$, the contact-ion pair $Na_2(H_3Si)_2P_4$, the neutral compound H_4P_4, and the silylated derivative $H_2(H_3Si)_2P_4$ (i.e., *trans*-2-tetraphosphene dianion $[HPPPPH]^{2-}$ (**10**), *cis*-2-tetraphosphene dianion $[HPPPPH]^{2-}$ (**11**), dianion $[H_2P_4]^{2-}$ with phosphanylcyclotriphosphane structure (**12**), dianion $[H_2P_4]^{2-}$ with cyclotetraphosphane structure (**13**), *trans*-2-tetraphosphene dianion $[(H_3Si)PPPP(SiH_3)]^{2-}$ (**14**), *cis*-2-tetraphosphene dianion $[(H_3Si)PPPP(SiH_3)]^{2-}$ (**15**), dianion $[(H_3Si)_2P_4]^{2-}$ with phosphanylcyclotriphosphane structure (**16**), dianion $[(H_3Si)_2P_4]^{2-}$ with cyclotetraphosphane structure (**17**), *trans*-2-tetraphosphene contact-ion pair $(H_3Si)NaPPPPNa(SiH_3)$ (**18**), *cis*-tetraphosphene contact-ion pair $(H_3Si)NaPPPPNa(SiH_3)$ (**19**), contact-

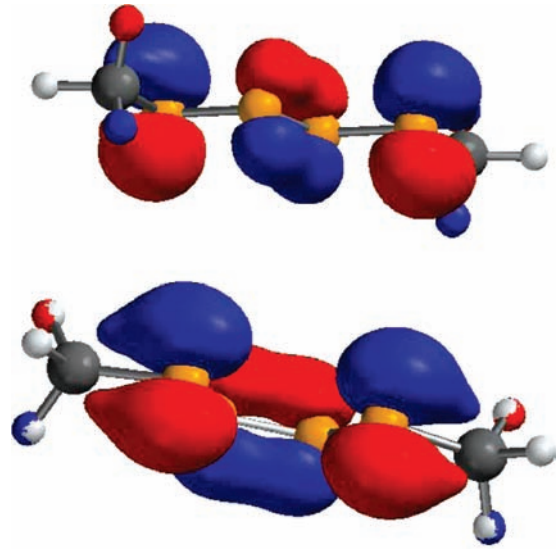

Figure 10. The π^* MOs of **14** and **15** calculated at the HF/6-311G(d)//B3LYP/6-31G(d) level (HOMO).

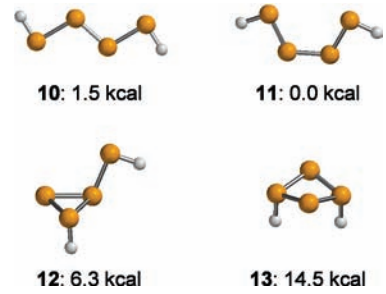

Figure 11. Calculated molecular structures of isomers **10**, **11**, **12**, and **13** of the dianion $[H_2P_4]^{2-}$ with the compound method G3.

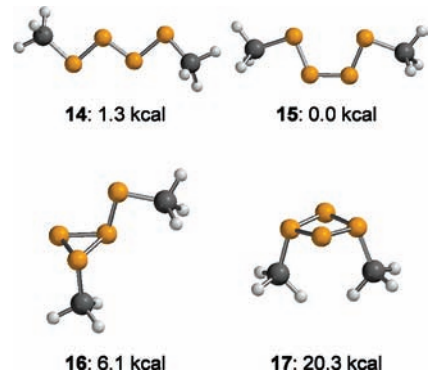

Figure 12. Calculated molecular structures of isomers **14**, **15**, **16**, and **17** of the dianion $[(H_3Si)_2P_4]^{2-}$ with the compound method G3.

(33) Schrödel, H.-P.; Nöth, H.; Schmidt-Amelunxen, M.; Schoeller, W.; Schmidpeter, A. *Chem. Ber./Recl.* **1997**, *130*, 1801.

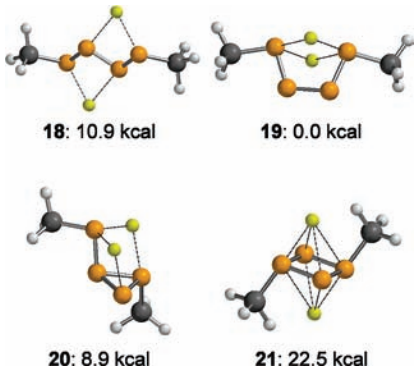

Figure 13. Calculated molecular structures of isomers **18**, **19**, **20**, and **21** of the contact-ion pair $(H_3Si)_2P_4Na_2$ with the compound method G3.

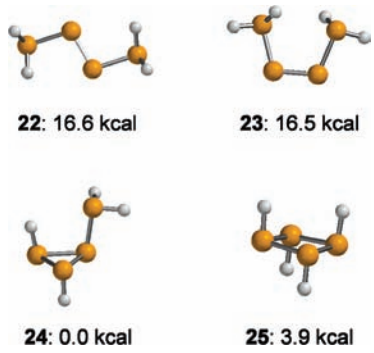

Figure 14. Calculated molecular structures of isomers **22**, **23**, **24**, and **25** of the neutral compound $[H_4P_4]$ with the compound method G3.

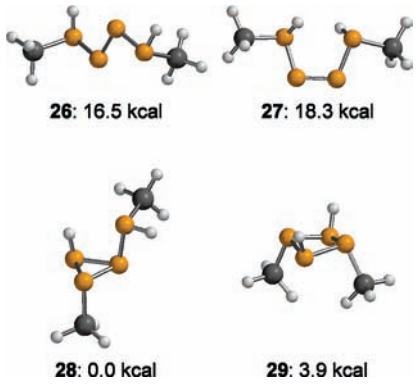

Figure 15. Calculated molecular structures of isomers **26**, **27**, **28**, and **29** of the neutral compound $[H_2(H_3Si)_2P_4]$ with the compound method G3.

ion pair $Na_2(H_3Si)_2P_4$ with phosphanylcyclotriphosphane structure (**20**), contact-ion pair $Na_2(H_3Si)_2P_4$ with cyclotetraphosphane structure (**21**), *trans*-2-tetraphosphene $H_2P-P=P-PH_2$ (**22**), *cis*-2-tetraphosphene $H_2P-P=P-PH_2$ (**23**), the neutral cyclic isomer of H_4P_4 with a phosphanylcyclotriphosphane structure (**24**), H_4P_4 with cyclotetraphosphane structure (**25**), *trans*-2-tetraphosphene $(H_3Si)HP-P=P-PH(SiH_3)$ (**26**), *cis*-2-tetraphosphene $(H_3Si)HP-P=P-PH(SiH_3)$ (**27**), the neutral cyclic isomer of $H_2(H_3Si)_2P_4$ with phosphanylcyclotriphosphane structure (**28**), and $H_2(H_3Si)_2P_4$ with cyclotetraphosphane structure (**29**)).

Figure 10 exemplarily shows the HOMOs of the silylated tetraphosphene dianions **14** and **15**. These orbitals, which are comparable to those of the ion-separated supersilylated tetraphosphenediide $[\mathbf{1}]^{2-}$, largely comprise (P_1,P_2) and (P_3,P_4) antibonding and (P_2,P_3) bonding contributions of the constituting p_z orbitals located at the chain of P atoms.

The results for the parent dianions $[H_2P_4]^{2-}$ and $[(H_3Si)_2P_4]^{2-}$ reveal a general thermodynamic preference for the formation of the respective acyclic ions. The ion-separated cis and trans forms **10** and **11** and **14** and **15** are significantly more stable than the cyclic isomers **12**, **13** or **16**, **17**. Further, the *cis*-tetraphosphenediides (**11** and **15**) are slightly more stable than the corresponding trans forms (**10** and **14**) (by 1.5 kcal/mol (**11**) or 1.3 kcal/mol (**15**), respectively; cf. Figures 11 and 12). Sodium coordination in $Na_2(H_3Si)_2P_4$ alters the energetic ordering of isomers dramatically (cf. Figure 13). First, we note that it increases the preference for the cis configuration significantly (i.e., *cis*-$Na_2(H_3Si)_2P_4$ **19** is 10.9 kcal/mol more stable than *trans*-$Na_2(H_3Si)_2P_4$ **18**). Moreover, the sodium contact-ion pair **20**, with its phosphanylcyclotriphosphane structure, becomes more stable than the trans-configured **18** and **21**, with its cyclotetraphosphane structure.

In contrast to the dianions $[H_2P_4]^{2-}$ and $[(H_3Si)_2P_4]^{2-}$, their neutral counterparts H_4P_4 and $H_2(H_3Si)_2P_4$ prefer the cyclic forms **24** and **28**. As shown in Figures 14 and 15, the ring compounds are much more stable than the acyclic isomers **22**, **23** and **26**, **27**.

These theoretical findings agree very well with our experimental observations: the anionic disupersilylated tetraphosphenediide derivatives possess an acyclic unsaturated structure, whereas their neutral tetraphosphene derivatives undergo isomerization reactions to form cyclic tetraphosphanes (e.g., **6** and **9**). We can, thus, relate these observations to general thermodynamic preferences inherent to the parent tetraphosphane framework.

Summary and Conclusion

In summary, we have shown that the tetraphosphenediides M_2[**1**] (M = Li, Na, K) can be prepared from precursor silanides M[Si-*t*-Bu_3] (M = Li, Na, K) via P_4 degradation, whereas the tetraphosphenediides M_2[**1**] (M = Rb, Cs) and Ba[**1**] are accessible by reaction of Na_2[**1**] with RbCl, CsF, and BaI_2, respectively. ^{31}P NMR experiments reveal that, in THF, Na_2[**1**] adopts a cis configuration. However, treatment of Na_2[**1**] with 18-crown-6 leads to the formation of [Na(18-crown-6)$(thf)_2]_2$[**1**] that possesses a trans configuration in the solid state. The ion-separated tetraphosphenediide [Na(18-crown-6)$(thf)_2]_2$[**1**] was characterized by X-ray crystallography. Addition of AuI to Na_2[**1**] yields 1,3-diiodo-2,4-disupersilyl-cyclotetraphosphane, which is an isomer of disupersilylated diiodotetraphosphene. A further isomer of disupersilylated tetraphosphene, the 3,5-disupersilyl-2,2-di-*tert*-butyl-2-stanna-bicyclo[2.1.$0^{1,4}$]pentaphosphane that possesses a phosphanylcyclotriphosphane structure, was obtained by the reaction of Na_2[**1**] with *t*-Bu_2SnCl_2. In contrast to analogous nitrogen compounds that consist of N_4 chains in cis or trans configuration, neutral 2-tetraphosphenes of the type *t*-$Bu_3SiRP-P=P-PR'Si$-*t*-Bu_3, with covalent RP and R′P bonds, seem to be less stable. On the one hand, tetraphosphenes *t*-$Bu_3SiRP-P=P-PR'Si$-*t*-Bu_3 with bulky R and R′ substituents undergo isomerization reactions with

the formation of isolable phosphanylcyclotriphosphane and cyclotetraphosphane derivatives (e.g., **9** (R = R′ = *t*-Bu_2Sn); **6** (R = I, R′ = I); Schemes 3 and 5), and on the other hand, decomposition of the protonated disupersilylated *cis*- and *trans*-tetraphosphene (R = H, R′ = H) occurs in the formation of *t*-Bu_3SiPH_2. In addition, the reactivity of Na_2[**1**] toward the Lewis acids BH_3 and $AlMe_3$ has been studied by heteronucleus NMR spectroscopy and mass spectrometry.

High-level quantum chemical calculations reveal that the acyclic cis and trans dianions of $[HPPPPH]^{2-}$ and $[H_3SiPPPPSiH_3]^{2-}$, **10** and **11**, as well as **14** and **15**, respectively, are thermodynamically favored over the cyclic phosphanylcyclotriphosphane or tetracyclophosphane isomers. However, upon sodium coordination in $Na_2(H_3Si)_2P_4$, the preference for cis configuration increases significantly. In contrast to the corresponding dianions, the neutral cyclic isomers of H_4P_4 and $H_2(H_3Si)_2P_4$, **24**, **25**, **28**, and **29**, are in turn significantly more stable than the isomers **22**, **23**, **26**, and **27** with their acyclic tetraphosphene units. It is interesting to note that the MOs of the silylated tetraphosphene dianions **14** and **15**, which are comparable with those of the ion-separated supersilylated tetraphosphenediide $[\mathbf{1}]^{2-}$ calculated at the HF/6-311G(d)//B3LYP/6-31G(d) level, show a highest occupied antibonding π * MO (HOMO). Therefore, the supersilylated tetraphosphene dianion shows promise as a non-innocent ligand for potentially redox-active transition-metal complexes.

Experimental Section

Quantum Chemical Calculations. Quantum chemical calculations were carried out by means of the Gaussian 03 program.[34] The thermochemical quantities for the different structures were calculated with the compound methods G3[35] and CBS-QB3,[36] as implemented in Gaussian 03. Relative energies (E_{rel}) refer to 1 atm in kcal/mol. We verified the minimum nature of the isomers reported by inspection of the Hessian matrices computed as part of the G3 and CBS-QB3 compound methods (positive eigenvalues of the diagonalized Hessian matrices for all species reported).

General Considerations. All experiments were carried out under dry argon or nitrogen using standard Schlenk and glovebox techniques. Alkane solvents were dried over sodium and freshly distilled prior to use. Toluene and THF were distilled from sodium/benzophenone. C_6D_6 was dried over molecular sieves and stored under dry nitrogen. $Li(thf)_3$[Si-*t*-Bu_3],[9] Na[Si-*t*-Bu_3],[19,22] and Na_2[**1**][14] were prepared according to published procedures. All other starting materials were purchased from commercial sources and used without further purification. NMR spectra were recorded on a Bruker AM 250, a Bruker DPX 250, a Bruker Avance 300, and a Bruker Avance 400 spectrometer. The ^{29}Si NMR spectra were recorded using the INEPT pulse sequence with empirically optimized parameters for polarization transfer from the *tert*-butyl substituents. Elemental analyses were performed at the microanalytical laboratories of the Universität Frankfurt. Mass spectrometry was performed with a Fisons VG Platform II, a Varian CH7, and a Kratos MS 80 RFA instrument. UV−vis absorption spectroscopy was carried out in THF using a Varian Cary 50 scan spectrophotometer.

[Na(18-crown-6)(thf)$_2$]$_2$[1]. To a solution of Na_2[**1**] (2.0 mmol) in 20 mL of THF was added 18-crown-6 (0.54 g, 2.1 mmol) in one portion. The purple solution was stirred overnight. Slow evaporation of the solvent yielded the product as crystalline dark violet plates (0.58 g, 53%). ^{1}H NMR (THF-d_8, internal TMS): δ 1.08 (br, *t*-Bu). ^{13}C{^{1}H} NMR (THF-d_8, internal TMS): δ 25.2 (br, *C*Me$_3$), 32.2 (br, C*Me$_3$*). ^{31}P{^{1}H} NMR: (see Figures 2 and 3).[37] ^{29}Si{^{1}H} NMR (THF-d_8, external TMS): (see Figure 5). UV−vis: λ_{max} = 494 nm, 561 nm.

Li$_2$[1]. A solution of $Li(thf)_3$[Si-*t*-Bu_3] (3.30 mmol) in 6.5 mL of THF was added dropwise to a cooled solution of P_4 (1.50 mmol) in 15 mL of THF. The reaction solution was warmed up to room temperature. Slow evaporation of the solvent yielded the tetraphosphenediide Li_2[**1**] as crystalline purple blocks (57%). Several attempts to determine the structure failed. ^{1}H NMR (THF-d_8, internal TMS): δ 1.06 (br, 54H, *t*-Bu). ^{13}C{^{1}H} NMR (THF-d_8, internal TMS): δ 25.0 (br, *C*Me$_3$), 32.1 (br, C*Me$_3$*). ^{31}P{^{1}H} NMR: (see Figure 2).[37] ^{29}Si{^{1}H} NMR (THF-d_8, external TMS): δ 21.8 (m).

Synthesis of the Tetraphosphenediides M$_2$[1] (M = Rb, Cs) and Ba[1]. A flask was charged with alkali-metal or alkaline-earth-metal halides (RbCl: 0.120 g, 1.12 mmol; CsF: 0.064 g, 0.44 mmol; BaI_2: 0.062 g, 0.16 mmol) to which was added a solution of an equimolar amount of a 0.1 M solution of Na_2[**1**] in THF (Rb: 5.6 mL, Cs: 2.2 mL, Ba: 1.6 mL). After 48 h at room temperature, the products were obtained in solution. Filtration and concentration of the filtrate yielded the microcrystalline purple tetraphosphenediides.

Rb$_2$[1]. ^{1}H NMR (THF-d_8, internal TMS): δ 1.09 (br, *t*-Bu). ^{13}C{^{1}H} NMR (THF-d_8, internal TMS): δ 25.3 (br, *C*Me$_3$), 32.2 (br, C*Me$_3$*). ^{31}P{^{1}H} NMR: (see Figure 2). ^{29}Si{^{1}H} NMR (THF-d_8, external TMS): δ 25.2 (m). An element ratio of Rb to P of 1:2.3 was determined by EDX spectrometry. Anal. Calcd for Rb_2[**1**](thf)$_2$ $C_{32}H_{70}O_2P_4Rb_2Si_2$: C, 45.87%; H, 8.42%. Found: C, 42.13%; H, 8.02%.

Cs$_2$[1]. ^{1}H NMR (THF-d_8, internal TMS): δ 1.08 (br, *t*-Bu). ^{13}C{^{1}H} NMR (THF-d_8, internal TMS): δ 25.1 (br, *C*Me$_3$), 32.3 (br, C*Me$_3$*). ^{31}P{^{1}H} NMR: (see Figure 2). ^{29}Si{^{1}H} NMR (THF-d_8, external TMS): δ 22.8 (m). (ESI$^+$) (%) (M = Cs$_2$[**1**](thf)$_2$) *m/z*: $[M]^+$ 932 (<5), $[M - Me]^+$ 917 (<5), [*t*-Bu_2MeSiPCsPPCsPSiMe-*t*-Bu_2]$^+$ 697 (10), $[Cs]^+$ 132 (100). An element ratio of Cs to P of 1:2.4 was determined by EDX spectrometry. Anal. Calcd for Cs_2[**1**](thf)$_2$ $C_{32}H_{70}O_2P_4Cs_2Si_2$: C, 41.20%; H, 7.56%. Found: C, 39.84%; H, 6.85%.

Ba[1]. ^{1}H NMR (THF-d_8, internal TMS): δ 1.09 (br, *t*-Bu). ^{13}C{^{1}H} NMR (THF-d_8, internal TMS): δ 25.2 (br, *C*Me$_3$), 32.4 (br, C*Me$_3$*). ^{31}P{^{1}H} NMR: δ 428.9, 19.0. ^{29}Si{^{1}H} NMR (THF-

(34) Frisch, M. J.; Trucks, G. W.; Schlegel, H. B.; Scuseria, G. E.; Robb, M. A.; Cheeseman, J. R.; Montgomery, J. A., Jr.; Kudin, K. N.; Burant, J. C.; Millam, J. M.; Iyengar, S. S.; Tomasi, J.; Barone, V.; Mennucci, B.; Cossi, M.; Scalmani, G.; Rega, N.; Petersson, G. A.; Nakatsuji, H.; Hada, M.; Ehara, M.; Toyota, K.; Fukuda, R.; Hasegawa, J.; Ishida, M.; Nakajima, T.; Honda, Y.; Kitao, O.; Nakai, H.; Klene, M.; Li, X.; Knox, J. E.; Hratchian, H. P.; Cross, J. B.; Bakken, V.; Adamo, C.; Jaramillo, J.; Gomperts, R.; Stratmann, R. E.; Yazyev, O.; Austin, A. J.; Cammi, R.; Pomelli, C.; Ochterski, J. W.; Ayala, P. Y.; Morokuma, K.; Voth, G. A.; Salvador, P.; Dannenberg, J. J.; Zakrzewski, V. G.; Dapprich, S.; Daniels, A. D.; Strain, M. C.; Farkas, O.; Malick, D. K.; Rabuck, A. D.; Raghavachari, K.; Foresman, J. B.; Ortiz, J. V.; Cui, Q.; Baboul, A. G.; Clifford, S.; Cioslowski, J.; Stefanov, B. B.; Liu, G.; Liashenko, A.; Piskorz, P.; Komaromi, I.; Martin, R. L.; Fox, D. J.; Keith, T.; Al-Laham, M. A.; Peng, C. Y.; Nanayakkara, A.; Challacombe, M.; Gill, P. M. W.; Johnson, B.; Chen, W.; Wong, M. W.; Gonzalez, C.; Pople, J. A. *Gaussian 03*; Gaussian, Inc.: Wallingford, CT, 2004.
(35) Curtiss, L. A.; Raghavachari, K.; Redfern, P. C.; Rassolov, V.; Pople, J. A. *J. Chem. Phys.* **1998**, *109*, 7764.
(36) Montgomery, J. A.; Frisch, M. J.; Ochterski, J. W.; Petersson, G. A. *J. Chem. Phys.* **1999**, *110*, 2822.

(37) Iterative optimization of the simulated spectrum with the software SpinWorks 2.5.5 yields the shown coupling constants. Marat, K. *SpinWorks 2.5.5*; University of Manitoba: Winnipeg, MB, 2006.

d_8, external TMS): δ 24.3 (m). An element ratio of Ba to P of 1:4.3 was determined by EDX spectrometry. Anal. Calcd for Ba[**1**](thf)$_2$C$_{32}$H$_{70}$BaO$_2$P$_4$Si$_2$: C, 47.79%; H, 8.77%. Found: C, 45.14%; H, 8.28%.

Protonolysis of M$_2$[1] (M = Li, Na, Rb, Cs) and Ba[1]. The tetraphosphenediides M$_2$[**1**] (M = Li, Na, Rb, Cs) and Ba[**1**] were treated with an excess of trifluoroacetic acid in THF (Li$_2$[**1**]: 0.5 mol, Na$_2$[**1**]: 2.0 mmol, Rb$_2$[**1**]: 0.1 mmol, Cs$_2$[**1**]: 0.1 mmol, Ba[**1**]: 0.1 mmol). As determined by ^{31}P NMR spectroscopy, the tetraphosphenediides are converted into supersilyl phosphane *t*-Bu$_3$SiPH$_2$ and, up to now, not exactly identified polyphosphanes. The ^{31}P signals of these polyphosphanes are very broad. By sublimation at 80 °C/0.01 mbar, pure *t*-Bu$_3$SiPH$_2$ was obtained as a waxy solid from the reaction of Na$_2$[**1**] with trifluoroacetic acid (yield 60%).

***t*-Bu$_3$SiPH$_2$.** ^{1}H NMR (C$_6$D$_6$, internal TMS): δ 0.94 (d, $^1J_{PH}$ = 185.4 Hz, 2 H), 1.09 (d, $^4J_{PH}$ = 0.49 Hz, 3 *t*-Bu). ^{13}C{^{1}H} NMR (C$_6$D$_6$, internal TMS): δ 23.1 (d, $^2J_{CP}$ = 5.86 Hz, *C*Me$_3$), 30.7 (d, $^3J_{PC}$ = 2.44 Hz, C*Me$_3$*). ^{31}P NMR (C$_6$D$_6$, external H$_3$PO$_4$): δ −263.8 (t, $^1J_{PH}$ = 185.4 Hz). ^{29}Si{^{1}H} NMR (C$_6$D$_6$, external TMS): δ 24.1 (d, $^1J_{PP}$ = 33.2 Hz). MS (EI) *m*/*z*: [M]$^+$ 232. Anal. Calcd for C$_{12}$H$_{29}$PSi: C, 62.01%; H, 12.58%. Found: C, 62.24%; H, 12.72%.

Remark: A mixture of sodium phosphides Na$_2$[**1**], Na$_4$[**2**], Na$_3$[**3**], Na[**4**], Na$_2$[**5**], Na[PHSi-*t*-Bu$_3$], and Na$_2$[PSi-*t*-Bu$_3$] in THF was titrated with trifluoroacetic acid (^{31}P NMR spectroscopic control). In the ^{31}P NMR spectra, the signals that can be assigned to Na$_2$[PSi-*t*-Bu$_3$] disappeared first, followed by those that can be assigned to the saturated phosphanides Na[PHSi-*t*-Bu$_3$], Na$_4$[**2**], Na$_3$[**3**], and Na$_2$[**5**], and, last, those that can be assigned to the unsaturated phosphides Na$_2$[**1**] and Na[**4**].

Oxidation of M$_2$[1] (M = Li, Na, Rb, Cs) and Ba[1]. Oxidation by equimolar amounts of TCNE and THF solutions of the tetraphosphenediides M$_2$[**1**] (M = Li, Na, Rb, Cs) and Ba[**1**] yielded the bicyclo[1.1.0]tetraphosphane (*t*-Bu$_3$Si)$_2$P$_4$ quantitatively, as determined by NMR spectroscopy (Li: 0.5 mol, Na: 2.0 mmol, Rb: 0.1 mmol, Cs: 0.1 mmol, Ba: 0.1 mmol). The bicyclo[1.1.0]tetraphosphane (*t*-Bu$_3$Si)$_2$P$_4$ could be freed of byproduct by removal of the THF solvent, extraction with pentane, and filtration.

Bicyclo[1.1.0]tetraphosphane (*t*-Bu$_3$Si)$_2$P$_4$. ^{1}H NMR (C$_6$D$_6$, internal TMS): δ 1.21 (br, *t*-Bu). ^{13}C{^{1}H} NMR (C$_6$D$_6$, internal TMS): δ 26.3 (br, *C*Me$_3$), 31.7 (br, C*Me$_3$*). ^{31}P{^{1}H} NMR (C$_6$D$_6$, external H$_3$PO$_4$): δ −139.1 (t, P−Si-*t*-Bu$_3$. ^1J_P = 170.5 Hz); δ −334.4 (t, PP$_3$, $^1J_{PP}$ = 170.5 Hz). ^{29}Si{^{1}H} NMR (C$_6$D$_6$, external TMS): δ 16.4 (m, Si-*t*-Bu$_3$). MS (EI) *m*/*z*: [M]$^+$ 251. Anal. Calcd for C$_{24}$H$_{54}$P$_4$Si$_2$: C, 55.14%; H, 10.41%. Found: C, 54.66%; H, 10.32%.

Reaction of Na$_2$[1] with BH$_3$. A 1.0 M solution of BH$_3$ (1.5 mmol) in 1.5 mL of THF was added dropwise to 7 mL of a 0.1 M solution of Na$_2$[**1**] (0.7 mmol) in THF at −80 °C. The purple solution was stirred for 1 h at −80 °C. From this solution, ^{31}P NMR spectra were measured at −80 and −50 °C and at room temperature, as shown in Figure 4. The reaction solution was slowly warmed up to room temperature. After 2 days, the color had changed from purple to yellow-orange, and, in the ^{31}P NMR spectrum, the signals of **8** had disappeared completely. In the ^{11}B NMR spectrum, a main signal occurred that can be assigned to Na[BH$_4$], and, in the ^{31}P NMR spectrum of this reaction mixture, new resonances in the range of saturated P atoms were found. ^{11}B NMR (THF-d_8, external BF$_3$·OEt$_2$): δ −41.5 (quint, Na[BH$_4$], $^1J_{BH}$ = 81.0 Hz), −36.5 (br m, **7**(BH$_3$)$_2$). ^{31}P{^{1}H} NMR: (see Figure 3).[37] After 2 days, ^{31}P NMR (THF-d_8, external H$_3$PO$_4$): δ −30.1 (m, (*t*-Bu$_3$Si)$_3$P$_7$), −113.0 (m, (*t*-Bu$_3$Si)$_3$P$_7$), −177.4 (m, (*t*-Bu$_3$Si)$_3$P$_7$), −139.1 (t, (*t*-Bu$_3$Si)$_2$P$_4$, $^1J_{PP}$ = 170.5 Hz), −334.4 (t, $^1J_{PP}$ = 170.5 Hz), −102.3 (m), −158.3 (br m), −188.0 (br m), −205.6 (m). In addition, we made a further experiment (BH$_3$: mmol, Na$_2$[**1**]: 0.7 mmol in mL of THF) to study the reaction of Na$_2$[**1**] with BH$_3$ by mass spectrometry. In the ESI$^-$ mass spectrum, we found peaks from [*t*-Bu$_3$SiP(BH$_3$)PPHP(BH$_3$)Si-*t*-Bu$_3$]$^-$. At first, obviously, the adduct **7**(BH$_3$)$_2$ is formed by the reaction between Na$_2$[**1**] and BH$_3$. Therefore, the signals of the ^{31}P NMR spectrum at −50 °C in Figure 4 can be assigned to the adduct **7**(BH$_3$)$_2$. The ESI$^-$ mass spectrum of the reaction solution reveals a further peak that can be assigned to [M + H]$^-$ of **8**(THF)$_2$.

7(BH$_3$)$_2$. ^{31}P NMR (THF-d_8, external H$_3$PO$_4$): (see Figure 4). (ESI) (%) *m*/*z*: 553.6 (14.6), 552.6 (36.6), 551.6 (100), 550.6 (72 interference with peaks of [*t*-Bu$_3$SiP(BH$_3$)PPP(BH$_3$)Si-*t*-Bu$_3$]$^-$ and [*t*-Bu$_3$SiP(BH$_3$)PPP(BH$_2$)Si-*t*-Bu$_3$]$^-$), 549.6 (93 interference with peaks of [*t*-Bu$_3$SiP(BH$_3$)PPP(BH$_3$)Si-*t*-Bu$_3$]$^-$ and [*t*-Bu$_3$SiP(BH$_3$)-PPP(BH$_2$)Si-*t*-Bu$_3$]$^-$, [*t*-Bu$_3$SiP(BH$_3$)PPHP(BH$_3$)Si-*t*-Bu$_3$]$^-$), calcd for [*t*-Bu$_3$SiP(BH$_3$)PPHP(BH$_3$)Si-*t*-Bu$_3$]$^-$ 553.4 (12.0), 552.4 (35.2), 551.3 (100), 550.4 (50.3), 549.4 (6.2), 548.6 (50.2 interference with a peak of [*t*-Bu$_3$SiP(BH$_3$)PPP(BH$_2$)Si-*t*-Bu$_3$]$^-$), calcd for [*t*-Bu$_3$SiP(BH$_3$)-PPP(BH$_3$)Si-*t*-Bu$_3$]$^-$ 552.4 (12.0), 551.4 (35.2), 550.3 (100), 549.4 (50.3), 548.4 (6.2), 547.5 (10.3), [*t*-Bu$_3$SiP(BH$_3$)PPP(BH$_3$)Si-*t*-Bu$_3$]$^-$, calcd for [*t*-Bu$_3$SiP(BH$_3$)PPP(BH$_2$)Si-*t*-Bu$_3$]$^-$ 553.4 (12.0), 552.4 (35.2), 551.3 (100), 550.4 (50.3), 547.4 (6.2).

8. ^{31}P NMR (THF-d_8, external H$_3$PO$_4$): δ 409.7, −35.0 (m, $^1J_{P(2)P(3)}$ = −507.0 Hz, $^1J_{P(1)P(2)}$ = −429.9 Hz, $^2J_{P(1)P(3)}$ = −35.4 Hz, $^3J_{P(1)P(4)}$ = 188.9 Hz, see Figure 4).[37] ^{11}B NMR (THF-d_8, external BF$_3$·OEt$_2$): δ −36.5 (br m, **7**(BH$_3$)$_2$). (ESI$^-$) (%) (M = **8**(thf)$_2$) *m*/*z*: [M + H]$^-$ 706.6 (10), 705.6 (34.8), 704.6 (48.4), 703.5 (100), 702.6 (34.9), calcd for [M + H]$^-$ 706.4 (4), 705.4 (16.3), 704.4 (44.8), 703.4 (100), 702.4 (22.2).

Reaction of Na$_2$[1] with AlMe$_3$. A 2.0 M solution of AlMe$_3$ (1.0 mmol) in 0.5 mL of THF was added dropwise to 6.2 mL of a 0.08 M solution of Na$_2$[**1**] in THF at −100 °C. The purple solution was stirred for 4 h at −100 °C. The reaction solution was warmed up to room temperature overnight. The ^{31}P NMR spectrum of this solution showed a signal that can be assigned to **7**(AlMe$_3$)$_2$ (Figure 2). After 1 week, the color had changed from purple to yellow-orange, and, in the ^{31}P NMR spectrum, the signal of **7**(AlMe$_3$)$_2$ had disappeared completely. The ^{31}P NMR spectrum of this reaction mixture revealed new resonances in the range of saturated P atoms. After 2 days, ^{31}P NMR (THF-d_8, external H$_3$PO$_4$): δ −87.7 (s, *t*-Bu$_3$SiPMe$_2$), −164.1 (d, *t*-Bu$_3$SiPHMe), −136.3(m), −184.2 (m), −212.5 (m), −231.4 (m)). In addition, we made a further experiment (AlMe$_3$: mmol, Na$_2$[**1**]: 0.7 mmol in mL of THF) to study the reaction of Na$_2$[**1**] with AlMe$_3$ by mass spectrometry. We found peaks in the ESI$^-$ mass spectrum that can be assigned to the adduct **7**(AlMe$_3$)$_2$.

7(AlMe$_3$)$_2$. ^{31}P NMR (THF-d_8, external H$_3$PO$_4$): δ 409.2 (m, $^1J_{P(2)P(3)}$ = −509.8 Hz, $^1J_{P(1)P(2)}$ = −434.3 Hz, $^2J_{P(1)P(3)}$ = −3.7 Hz, $^3J_{P(1)P(4)}$ = 162.4 Hz, see Figure 5). (ESI$^-$) (%) (M = **7**(AlMe$_3$)$_2$(thf)$_5$) *m*/*z*: [M]$^-$ 1074.7 (68), 1073.9 (100), 1072.7 (90), calcd for [M]$^-$ 1074.6 (29), 1073.7 (66), 1072.6 (100).

Cyclotetraphosphane 6. A solution of Na$_2$[**1**] (1.5 mmol) in 15 mL of THF was added to solid AuI (0.49 g, 1.52 mmol). The red-brown solution was stirred overnight. After removal of the solvent under reduced pressure, the residue was extracted with toluene and filtered. Slow evaporation of the solvent yielded the product as yellow crystalline plates (47%). ^{1}H NMR (C$_6$D$_6$, internal TMS): δ 1.22 (br, *t*-Bu). ^{13}C{^{1}H} NMR (C$_6$D$_6$, internal TMS): δ 25.4 (br, *C*Me$_3$), 32.8 (br, C*Me$_3$*). ^{31}P{^{1}H} NMR): δ 149.0 (t, $^1J_{PP}$ = 226.7 Hz), −34.9 (t, $^1J_{PP}$ = 226.7 Hz). ^{29}Si{^{1}H} NMR (C$_6$D$_6$, external

TMS): δ 21.5 (m). MS (MALDI) (%) *m/z*: $[M]^+$ 776 (60), $[M - Si\text{-}t\text{-}Bu_3]^+$ 577 (100). Anal. Calcd for $C_{24}H_{54}I_2P_4Si_2$: C, 37.12%; H, 7.01%. Found: C, 37.31%; H, 7.18%.

Phosphanylcyclotriphosphane 9. To a solution of Na_2[**1**] (1.5 mmol) in 15 mL of THF was added $t\text{-}Bu_2SnCl_2$ (0.46 g, 1.5 mmol) in one portion. The solution quickly became cloudy, and the color changed from purple to yellow-orange. After 3 h, volatiles were removed in vacuo, and the residue was extracted with pentane (10 mL). The extract was filtered. Slow concentration of the filtrate led to the deposition of the product as a microcrystalline orange solid (64%). ^{1}H NMR (C_6D_6, internal TMS): δ 1.30 (br, 54H, Si-*t*-Bu_3), 1.28 (br, 18H, Sn-*t*-Bu_2). $^{13}C\{^1H\}$ NMR (C_6D_6, internal TMS): δ 22.6 (br, Sn*C*Me$_3$), 23.0 (br, Sn*C*Me$_3$), 25.5 (br, PSi*C*Me$_3$), 26.3 (br, SnPSi*C*Me$_3$), 30.1 (br, SnC*Me$_3$*), 30.6 (br, SnC*Me$_3$*), 31.8 (br, PSiC*Me$_3$*), 32.3 (br, SnPSiC*Me$_3$*). $^{31}P\{^1H\}$ NMR (C_6D_6, external TMS):[37] δ −105.3 (m, $^1J_{P(1)P(4)} = -280.2$ Hz, $^2J_{P(2)P(4)} = 74.6$ Hz, $^2J_{P(3)P(4)} = 16.8$ Hz, $^1J_{119SnP(4)} = 946.0$ Hz, $^1J_{117SnP(4)} = 905.0$ Hz, P(4)), −124.8 (m, $^1J_{P(1)P(2)} = -238.7$ Hz, $^1J_{P(1)P(3)} = -160.4$ Hz, $^2J_{119SnP(1)} = 197.1$ Hz, $^2J_{117SnP(1)} = 198.8$ Hz, P(1)), −180.4 (m, $^1J_{P(2)P(3)} = -147.9$ Hz, $^1J_{119SnP(3)} = 628.8$ Hz, $^1J_{117SnP(3)} = 600.6$ Hz, P(3)), −198.2 (m, $^2J_{119SnP(2)} = 122.0$ Hz, $^2J_{117SnP(2)} = 121.2$ Hz, P(2)). $^{29}Si\{^1H\}$ NMR (C_6D_6, external TMS): δ 19.1 (dm, $^1J_{PSi} = 95.1$ Hz, PSi-*t*-Bu_3), 26.4 (dm, $^1J_{PSi} = 89.9$ Hz, SnPSi-*t*-Bu_3). $^{119}Sn\{^1H\}$ NMR (C_6D_6, external TMS): δ 76.0 (m, $^1J_{119SnP(5)} = 946.0$ Hz, $^1J_{119SnP(3)} = 628.8$ Hz, $^2J_{119SnP(2)} = 122.0$ Hz, $^2J_{119SnP(1)} = 197.1$ Hz). (EI) (%) *m/z*: $[M - t\text{-}Bu_3Si - 2C_4H_8]^+$ 445 (100), 443 (72), 447 (41), 441 (34), 446 (30), 442 (25), 449 (17), 448 (8), calcd for $[M - t\text{-}Bu_3Si - 2C_4H_8]^+$ 445 (100), 443 (75.1), 447 (18), 441 (42.0), 446 (30), 442 (18), 449 (17), 448 (3). Anal. Calcd for $C_{32}H_{72}P_4Si_2Sn$: C, 50.86%; H, 9.60%. Found: C, 49.22%; H, 9.81%.

X-ray Structure Determination. The very large *R* values in the structure determination of $[Na(18\text{-crown-6})(thf)_2]_2$[**1**] are a result of the loose packing of the molecules. The large displacement parameters (*U* values of about 0.2) show the *t*-Bu groups and the crown ether rings to be disordered. The scattering power of the crystal is limited due to the large thermal motion. We tried several disorder models, but with no significant improvement of the results. The unit cell also contains two symmetry-related, solvent-accessible areas of 620 Å^3 each, corresponding to 22% of the unit cell volume, where no atoms were found. The residual density in these areas did not exceed 1 e/Å^3. Thus, the unit cell is expected to contain a large amount of solvate, though none was observable. The SQEEZE option in program PLATON was not used. The figures of merit are not satisfactory, but the structure determination unequivocally confirms the molecular structure and allows its discussion.

Data collections were performed on a Stoe-IPDS-II diffractometer and Siemens CCD three-circle diffractometer, with empirical absorption correction using MULABS[38] and SADABS.[39] The structures were solved with direct methods[40] and refined against F^2 by full-matrix least-squares calculations with SHELXL-97.[41] Hydrogen atoms were placed on ideal positions and refined with fixed isotropic displacement parameters using a riding model. CCDC reference numbers: 690493 ($[Na(18\text{-crown-6})(thf)_2]_2$[**1**]) and 690500 (**6**).

Acknowledgment. We are grateful to the Goethe-Universität Frankfurt for financial funding, and the Chemetall GmbH for a gift of *tert*-butyl lithium. A.L. and G.M. wish to thank the Fonds der Chemischen Industrie (FCI) and the Bundesministerium für Bildung and Forschung (BMBF) for Ph.D. grants. Computer time provided by the CSC Frankfurt and the HLR Darmstadt is acknowledged.

Supporting Information Available: Table of X-ray parameters, atomic coordinates, displacement parameters, and bond distances and angles. This material is available free of charge via the Internet at http://pubs.acs.org.

IC8016003

(38) Blessing, R. H. *Acta Crystallogr., Sect. A* **1995**, *51*, 33.
(39) Sheldrick, G. M. *SADABS*; University of Göttingen: Göttingen, Germany, 2000.
(40) Sheldrick, G. M. *Acta Crystallogr., Sect. A* **1990**, *46*, 467.
(41) Sheldrick, G. M. *SHELXL-97: A Program for the Refinement of Crystal Structures*; University of Göttingen: Gottingen, Germany, 1997.